BIOMORPHODYNAMICS OF ALTERNATE BARS IN A CHANNELIZED, REGULATED RIVER: AN INTEGRATED HISTORICAL AND MODELLING ANALYSIS

Alyssa J. Serlet[1,2,*], Angela M. Gurnell[2], Guido Zolezzi[1], Geraldene Wharton[2], Philippe Belleudy[3], Camille Jourdain[3]

[1] Dept. of Civil Environmental and Mechanical Engineering, University of Trento, Trento, Italy

[2] School of Geography, Queen Mary University of London, London E1 4NS, United Kingdom

[3] Univ. Grenoble Alpes, CNRS, IRD, Grenoble INP, IGE, F-38000 Grenoble, France

* corresponding author

ABSTRACT

The development of alternate bars in channelized rivers can be explained theoretically as an instability of the riverbed when the active channel width to depth ratio exceeds a threshold. However, the development of a vegetation cover on the alternate bars of some channelized rivers and its interactions with bar morphology have not been investigated in detail.

Our study focused on the co-evolution of alternate bars and vegetation along a 33 km reach of the Isère River, France. We analysed historical information to investigate the development of alternate bars and their colonization by vegetation

This article has been accepted for publication and undergone full peer review but has not been through the copyediting, typesetting, pagination and proofreading process which may lead to differences between this version and the Version of Record. Please cite this article as doi: 10.1002/esp.4349

within a straightened, embanked river subject to flow regulation, sediment mining, and vegetation management. Over an 80 year period, bar density decreased, bar length increased, and bar mobility slowed. Vegetation encroachment across bar surfaces accompanied these temporal changes and, once established, vegetation cover persisted, shifting the overall system from an unvegetated to a vegetated dynamic equilibrium state.

The unvegetated morphodynamics of the impressively regular sequence of alternate bars that developed in the Isère following channelization is consistent with previous theoretical morphodynamic work. However, the apparent triggering dynamics of vegetation colonization needs to be investigated, based on complex biophysical instability processes. If instability related to vegetation colonization is confirmed, further work needs to focus on the relevance of initial conditions for this instability, and on related feedback effects such as how the morphodynamics of bare-sediment alternate bars may have affected vegetation development and, in turn, how vegetation has created a new dynamic equilibrium state.

KEYWORDS

Channelization, alternate bars, biomorphodynamics, bar theory, vegetation encroachment, flow regulation, sediment mining

INTRODUCTION

Extensive channelization has affected many river systems worldwide including widespread levée construction which has occurred along European rivers since the mid 1800s (e.g. Petts, 1989) and is currently being widely implemented in many developing countries (e.g. Siviglia et al., 2008). The motivation for embankment construction varies from land reclamation to flood protection but it is almost invariably accompanied by a marked decrease in river channel width. Such confinement of river channels to a narrower width has dramatic effects on channel morphology (Garcia Lugo et al., 2015). While river channels prior to embanking and width reduction may have adopted a continuum of morphologies, following channelization, rather discontinuous responses have been observed, with distinct and often new morphological styles emerging. The piedmont reaches of many Alpine rivers in Europe offer several examples, with some reaches developing long, impressively regular, sequences of alternating bars (e.g. the Alpine Rhine, Jäggi, 1984, Adami et al., 2016), whereas bars are almost absent in others (e.g. the Rhone in Switzerland, Stäuble et al., 2008; the Alpine Rhine downstream of the Ill confluence, Adami et al., 2016 and the Adige in NE Italy, Scorpio et al., 2018). Following decades of mathematical theories concerning alternate bars (e.g. Tubino et al., 1999) supported by experimental work in laboratory flumes (e.g. Lanzoni, 2000) and, more recently, integration of these with observations on channelized rivers (e.g. Rodrigues et al., 2015, Jaballah et al., 2015, Adami et al., 2016), the marked differences in morphology can be robustly explained. Long sequences of alternate bars tend to form because of an inherent instability of the riverbed when the active channel width to depth ratio exceeds a threshold that depends on the reach-averaged hydraulic conditions. By viewing bar formation as an instability process and

recognizing the existence of a threshold for such instability to occur, the observed discontinuous morphological response of rivers to channelization and narrowing can be explained.

However, observations of channelized rivers with alternate bars reveal two additional states: vegetated and unvegetated (bare sediment) bars. The development of vegetation on alternate bars and its interactions with bar morphology do not appear to have been investigated in detail, although this phenomenon can be observed (e.g. on the French rivers Arc, Jaballah et al., 2015; Isère, Vautier, 2000; lower Drac, Google Maps, accessed April 16, 2017). While alternate bar development can be clearly related to channelization, controls on such biophysical interactions might also reflect many other human actions occurring within the same catchment, which can be investigated across a spectrum of temporal and spatial scales using a wide range of historical information sources (for a recent review see Grabowski et al., 2014) and integrating such analysis with modelling approaches (e.g. Scorpio et al., 2018).

When the aim is to investigate changes in river morphology occurring over recent decades, aerial photographs can provide information that extends back 100 years in some cases, with increasing temporal resolution offered by satellite data over the last three decades. Aerial images provide information on changes in river size (e.g. Liébault and Piégay, 2002), planform (e.g. Abate et al., 2015; Clerici et al., 2015; David et al., 2016; Magliulo et al., 2016), channel and floodplain geomorphic features (e.g. Adami et al., 2016) and vegetation cover (e.g. Asaeda and Rashid, 2012; Comiti et al., 2011; Molnar et al., 2008; Surian et al., 2015; Corenblit et al., 2016). Sequences of aerial images have also been employed to investigate morphodynamic responses to specific human activities that directly or indirectly affect fluvial processes. For example, direct effects on fluvial processes and their morphological

consequences arise from activities such as dam and weir construction (Choi et al., 2005; Kiss and Blanka, 2012) and removal (Woelfle-Erskine et al., 2012), channel realignment, embanking and reinforcement (Corenblit et al., 2016; Jaballah et al., 2015; Urban and Rhoads, 2003), river bed gravel mining (Rinaldi et al., 2005) and river restoration (Pasquale et al., 2011; Schirmer et al., 2014) whereas indirect effects can result from changes in land cover and land management within the river's catchment (González del Tánago et al., 2016; Grabowski and Gurnell, 2016; Liébault and Piégay, 2002; Provansal et al., 2014). By comparing time sequences of images, morphological responses to changes in processes can be identified and trajectories of changes can be characterized and interpreted (Belletti et al., 2016; David et al., 2016; Fryirs et al., 2009). When the outputs from historical analyses are compared with outputs from morphodynamic models such as that of Tealdi et al. (2011) or from laboratory experiments such as that of Garcia Lugo et al. (2015), further important advances can be achieved including the testing of theories, insight on the generalization of cause-effect linkages (e.g. Zolezzi et al., 2012, Rodrigues et al., 2015, Adami et al., 2016), as well as better identification and interpretation of causes and effects that may otherwise be difficult to identify and interpret because different actions may occur at similar times or locations (e.g. Provansal et al., 2014; Zanoni et al., 2008).

Our study investigated how human interventions may have affected the planform morphological trajectory of a reach of the River Isère, France, particularly the development of alternate bars within an embanked channel subject to flow regulation, sediment mining, and vegetation management. The Isère is known for having developed a rather rapid planform shift from bare gravel alternate bars to heavily vegetated alternate bars. However, previous studies (Didier, 1994; Vautier,

2000; Allain-Jegou, 2002; Alcayaga, 2013; Jourdain, 2017), have not quantified this transition either in terms of bar dynamics or biomorphological trajectory. Here we explicitly focus on the biomorphodynamics of alternate bars, and we take a long term (80 years) and reach-scale (>30 km) approach, to fully address the biomorphological trajectories that have occurred and link them to potential causes. We perform an analysis of historical aerial images, complemented by information from other documents and gauged flow records, and by the application of analytical morphodynamic models, based on the linear theories for free migrating and steady "spatial" bars (e.g. Colombini et al., 1987, Seminara and Tubino, 1992). By investigating planform morphological responses of the river to changes in different human stressors through time and in different parts of the reach, we quantitatively characterize and gain biophysical insights into the transition that occurred between gravel-bar and vegetated-bar states. The outcomes of this integrated historical and modelling analysis provide both site-specific and more general understanding of the impacts of particular human stressors, support biomorphodynamic modelling that addresses the mutual interplay among river morphology and riparian vegetation (e.g. Camporeale et al., 2013, Zen et al., 2016) and contribute to future management decision-making within regulated, channelized rivers where such interaction occurs.

THE STUDY AREA AND REACH

The River Isère, a tributary of the River Rhône, is located in southeast France. This research was conducted on a 33 km long reach of the river from Frontenex to Pontcharra (Figure 1), which includes the confluence with the River Arc. Two smaller tributaries are the Gelon (near Châteauneuf) and the Breda (near Pontcharra).

Figure 1: The location of the study reach of the River Isère showing the locations of major dams, interbasin transfers and sediment mining in and upstream of the study reach (where > 20000 m^3 of sediment were extracted during the mid-20th century).

The River Isère's natural flow regime is nivo-glacial with an average flow of 178 $m^3 s^{-1}$ at Grenoble (where river flows have been monitored throughout our 80 year study period) and high sediment transport (Vivian, 1969; Didier, 1994). Table 1 provides summary hydrological information for the river basin upstream of the Arc confluence at Albertville, downstream of the confluence at Montmélian and further downstream at Grenoble. Prior to channelization in the 19th century, the study reach was braided (Institut National de l'Information Géographique et Forestière, no date). For example, Figure 2 illustrates an island braided section near Montmélian in 1781-1782.

Table 1: Hydrological information on the river basin upstream of the Arc confluence at Albertville, downstream the confluence at Montmélian and further downstream in Grenoble

Figure 2: The River Isère near Montmélian in 1781-2, before channelization (source: the Marchetti map, Archives Départementales de la Savoie)

Major straightening and embanking of the River Isère was completed in 1858 (Clément, 2011; Girel, 2010) with several subsequent modifications and additions.

The channel width was designed to 175 m upstream and 225 m downstream of the Arc confluence (Clément, 2011), however the built embankments currently define a channel width of approximately 100 m upstream and between 120 and 140 m downstream. The longitudinal slope just upstream of the study reach (3 km upstream of Frontenex) is 0.0025 m/m and downstream (near Pontcharra) it is 0.0013 m/m. At an early stage after channelization, sediment supply was affected by torrent control works (Bravard, 1989). Mountain slope reforestation and check dams have reduced the sediment supply from the tributaries since the 1860s (Peiry et al., 1994).

Following channelization, the river developed a planform of alternate bars within the embanked channel. This planform has subsequently evolved over a period during which a range of other human interventions and pressures have affected the study reach. Hydropower development started as early as 1867 with the installation of chutes but the building of dams started in the early 20th century (Pupier, 1996; Ritter, 1959). The construction of the large Tignes reservoir in 1952 was the beginning of a very intensive construction period for hydropower dams (Figure 1). Additionally, two major inter-basin transfers were constructed between the Arc and Isère rivers. The Isère-Arc diversion (implemented in 1953) caused a drastic decrease in high and mean flows and consequently reduced bedload input upstream of the Arc confluence. The second large inter-basin transfer from the Arc to the Isère was implemented in 1980. In addition, there has been sediment mining of the river bed, which was particularly active from the late 1940s to the 1970s and ceased by 1980 (Figure 1). Since the 1980s sediment weirs have been installed for stabilizing the longitudinal profile of the Isère (Peiry et al., 1994), which may also have affected sediment transfer through the study reach. In addition, in different locations and at

different dates, colonizing vegetation has been removed from many bar surfaces to maintain conveyance of high flows.

METHODS

Information on the morphological evolution of the reach and possible influencing factors was extracted and analysed from three types of historical data sources covering the past 80 years: flow records; aerial images; historical documents. The historical analysis was then integrated with the application of analytical morphodynamic models for river bars.

Flow records

A long time series of daily flows gauged at Grenoble, approximately 40 km downstream from the study reach, were assembled for analysis. Records of daily flows from 1960 were downloaded from the official online hydrological databank "Banque HYDRO" of the French Ministry of Ecology, Sustainable Development and Energy. Earlier data from 1877 to 1968 were in the form of quite frequent but irregular stage measurements (Lang et al., 2003), which were converted to discharge using the formula proposed in Badel (2000). Daily discharges were estimated from these measurements, taking an average whenever more than one observation occurred in a day and using linear interpolation for days with missing data. Comparison of daily flow estimates in the 1960-1968 overlap period showed considerable variance around a linear regression relationship that revealed slight but increasing overestimation of the highest flows above approximately 400 $m^3 s^{-1}$ with notable overestimation when flows exceeded 600 $m^3 s^{-1}$ and slight underestimation

of the lowest flows. In order to support an integrated analysis, the earlier flow records were adjusted to be consistent with the recent records using a linear regression model estimated for the overlap period.

The adjusted flow records were used first to assess the discharge at the time of capture of the analysed aerial images and secondly to conduct an analysis relating water area in the images to flow in order to assess the degree to which river stage influenced the area that was inundated within the embanked channel. A third analysis investigated whether there was evidence for any changes in the discharge regime over the period of records using the IARI assessment method (Rinaldi et al., 2011). To achieve this, four time periods were considered (1905-1928, 1930-1950, 1960-1980, 1996-2016) which, after taking account of gaps in the record, yielded approximately 20 years of flow data in each period. An analysis of monthly mean flows was undertaken to reduce the likelihood of any significant impacts caused by remaining differences in the estimation of the highest daily flows and by the lower temporal resolution of the earlier flow records. Changes in the distribution of monthly mean discharges (specifically, the mean (MEAN_QmMEAN), maximum (MAX_QmMEAN) and minimum values (MIN_QmMEAN), and their coefficients of variation) were analysed.

Table 2: Dates, study reach coverage (in km from 1 (upstream) to 33 (downstream) along the study reach) and approximate spatial scale of the aerial images analysed, accompanied when available by the daily discharge monitored at Grenoble for the image date. (Note that precise dates are not available for all images, preventing the concurrent daily discharge from being estimated).

Aerial images

The aerial images that were analysed are listed in Table 2 (image source: Institut Géographique National), including their coverage of the 33 x 1 km sections of the study reach, their approximate spatial scale, and, when available, the estimated discharge at the time of image capture. The images date back to the 1930s, covering a period throughout which the river was channelized and embanked. The chosen images mainly reflect availability and coverage of the study reach. In particular, all images captured before the mid-1980s were analysed.

All image analysis was conducted using ArcGIS and AutoCAD. Each set of aerial images was geocorrected and georeferenced to the Lambert II projection. An analysis of the positional accuracy of a set of ground control points across the images was then undertaken to assess the degree to which this might affect analysis of feature movements through the time sequence of images.

The boundaries of the embanked channel and enclosed areas of exposed bare sediment, vegetation, and water were digitised so that the area of the embanked channel (total channel), water, bars (exposed bare sediment plus vegetation), bare bar surfaces (exposed bare sediment), and vegetated bar surfaces (vegetation) could be calculated for the entire study reach; the parts upstream and downstream of the Arc confluence (located at 12.5 km); and within each 1 km section of the 33 km reach. An analysis of the relationship between the water area and the estimated discharge at the time of image capture was undertaken to assess whether analysis of emergent bar dimensions would be adversely affected by differences in river stage. The areal estimates of channel, vegetation, exposed bare sediment, and water were then used to explore spatial and temporal changes in channel morphology. In addition, three 3 km subreaches were selected to investigate detailed

changes in the position of bar centroids across the time sequence of photographs. The annual changes in bar centroid positions along the entire 33 km reach were investigated for four short time periods that had good image coverage for the reach during the early (1936 to 1939), middle (1968-1969), later (1977-1978) and most recent parts of the investigated 80 year time period.

Bar polygon centroids were located using a geometric object snap function in AutoCAD. For centroid detection, the entire bar surfaces were digitized as polygons, each bar polygon including the vegetated and bare sediment portions of the same bar. When the bar surface was observed to include a wet channel much smaller than the main wet channel, this was not considered sufficient to split the corresponding bar polygon into two. Local bar migration rates were computed as the difference between the positions of bar centroids in two aerial images that were closely spaced in time, divided by the time in years between the two images. In addition, two measures of bar size were extracted. The length of each bar unit (’bar length‘) was computed as the distance between the bar unit head and tail, defined by the initial and final points at which the bar shoreline intercepted the bank. The ’bar wavelength‘ was computed as the distance between two adjacent bar centroids along the same river bank, and is a measure that is expected to be largely independent of water stage at the time of image capture. Bar wavelength comes from conceptualizing alternate bars as two-dimensional bed morphology waves. Bar wavelengths were scaled using the local averaged channel width to produce estimates that could be compared with those from other rivers and from analytical theories and numerical models.

Historical Documents

Information on three main human interventions and pressures relevant to the evolution of the morphology of the study reach was obtained from various reports and archives.

Information on hydropower development was obtained from Pupier (1996), Ritter (1959) and Vautier (2000). Data on sediment mining were obtained from the office of the “Archives départementales de la Savoie”. Although there were many documents concerning sediment removal from the late 1940s until the beginning of the 1970s, these are likely to provide an underestimate of total sediment removal because some documents may be missing and some stated quantities may be underestimated. Furthermore, sediment removal did not completely cease until around 1980 (Syndicat Mixte de l’Isère et de l’Arc Combe de Savoie, oral communication). Air photographs often provided supporting evidence on the locations and impacts of sediment removal. Although vegetation removal from bar surfaces is known to have been practiced, no formal records of the activity were located, and so the aerial images formed the main source of information on the timing and location of vegetation clearance (e.g. Figure 3).

Figure 3: Three aerial images showing the same bar fully vegetated (1967), after vegetation and sediment removal (1968), and a year later showing rapid early vegetation recovery (1969) at pont de Gresy, Aiton (km 7 of the study reach, flow right to left). Note that the dark shade of the entire surface of the bar beneath the bridge in the 1968 image is a result of vegetation and bar surface excavation and,

therefore, shows complete removal of the vegetation cover on the bar during 1968. (source images: Institut Géographique National)

Analytical morphodynamic theories

Analytical morphodynamic theories are mathematical models based on approximate solutions of the momentum and mass conservation equations for water and sediments that flow in an open channel with a movable bed (e.g. Callander, 1969). The mathematical model is kept at the lowest meaningful level of complexity through a series of simplifying assumptions which retain the key physical ingredients, despite strongly simplifying the actual heterogeneity characterizing natural rivers. These theories consider alternate bars as waves of the riverbed that are able to deform a plane bed configuration, and which would correspond to the uniform flow of a competent, formative streamflow, taken as a reference flow condition from which input parameters are computed.

The planform of the Isère study reach is straight for 89% of its length and it consists of a sequence of 7 straight longitudinal sections, connected by 5 short bends of constant curvature. In the present study we have therefore applied linear theories for alternate bars in straight river reaches, which predict conditions of formation, wavelength, and migration properties of alternate bars for given reach-averaged values of flow discharge, channel width, reach slope, and sediment grain size. Quantitative theoretical outcomes also depend on the choice of the hydraulic roughness formula and of the bedload predictor, for which a log-like formula and the Meyer-Peter and Müller (1948) relation have been used in our study.

Alternate bars can theoretically develop in straight reaches of equal width because of a free instability mechanism of the riverbed (thus called “free bars”, e.g. Tubino et al.,

1999) or can be forced by local persistent perturbations of the straight channel planform, like a bend or the Arc confluence in the case of the Isère (these are called “spatial bars”, Seminara and Tubino, 1992 or “hybrid bars”, Durò et al., 2016). Free migrating bars develop provided the width to depth ratio, β, under bar-forming conditions exceeds a threshold, β_c. Also, free bars are downstream migrating, while hybrid bars are nonmigrating. Besides the specific theoretical literature, further details on the application of such theories to field cases can be found in Zolezzi et al. (2012), Jaballah et al. (2013), Rodrigues et al. (2015), Adami et al. (2016) and Scorpio et al. (2018).

RESULTS

Potential sources of error in the analysis of river biomorphological features from aerial images

A first stage in the analysis was to consider the likely accuracy of the positions and dimensions of any morphological features extracted from the aerial images.

One potential source of error was the accuracy of image geocorrection and georeferencing. To estimate this, the most recent (2011) corrected image was used as a reference. Ten control points that were easy to identify and locate were used for the assessment of positional accuracy of all images. The positions of these points on the 2011 images were compared with their positions on all other images. 172 positional error estimates were obtained because not all control points were captured for all image dates. The average positional deviation of these points from 2011 was 8.4 m with a standard error of 0.5 m. Given the embanked channel width is approximately 100m in the section upstream of the Arc confluence and 120 to 140 m

downstream, these positional errors should be borne in mind when interpreting morphological changes but they are not sufficiently large to invalidate the intended analyses.

A second potential source of error in interpreting river morphological changes was the river stage at the time of image capture. To investigate this, the water area within 1 km sections of the study reach was plotted against the discharge at the time of image capture (Figure 4). There is considerable variance in the water area among 1 km sections for individual image dates, making data from images that capture only a small number of contiguous sections difficult to interpret. Nevertheless, there is some evidence for an increase in water area in the June 1970 image, when flow exceeded 400 m^3 s^{-1}, and data drawn from the 1936 and 1982 images show some concentration of observations towards the upper end of the range observed. Furthermore, when flow falls below 120 m^3 s^{-1} (October 1967, September 1969, August 1972, September 1978, and 3 images in August 1996), the water area across the recorded sections appears to decline slightly. However, when the image dates are plotted against the time series of daily flows from 1930 to 2016 (Figure 5), it is apparent that none were captured during particularly high flows and the majority were observed close to or below the average flow of 178 m^3 s^{-1}, measured at Grenoble. For this reason and because of the high variance among sections for each image date (Figure 4), the differences in the number and location of the 1 km sections captured within each image (Table 2) and the potential influence of the development of exposed bars through time on water area, we concluded that the variability in water level among the different images was unlikely to significantly affect our study and so none of the images was removed from the analysis.

Figure 4: Percentage of the embanked channel area occupied by water within the 1 km sections of the study reach captured by the available aerial images, plotted in relation to the daily discharge monitored at Grenoble on the day of image capture. (Note that not all sets of images cover the entire set of 33 1km sections)

Figure 5: Daily mean discharge at Grenoble, locating the times when the analysed aerial images were captured (note that high discharges, particularly those above 600 $m^3 s^{-1}$, are over-estimated in the records before 1960).

Figure 6: Percentage of embanked channel occupied by bars (exposed bare sediment and vegetated surfaces) and vegetated bars (vegetated surfaces only); and percentage of the active channel (water and exposed bare sediment) occupied by bars (exposed bare sediment) extracted from aerial images of different date covering (b) the entire 33 km study reach; (c) the study reach upstream of the River Arc confluence; and (d) the study reach downstream of the River Arc confluence. Data are presented for all image dates that provide complete or near-complete coverage of the relevant reach. The timing of implementation of the main human factors that may have influenced the biogeomorphic changes are indicated in (a), with the commencement of sediment mining, the activation of the Tignes hydropower dam, and the Isère-Arc and Arc-Isère diversions marked by vertical dashed lines.

Biomorphological river trajectories extracted from aerial images

The morphology of the study reach was characterized by alternate bars on all images. Image analysis was first undertaken across the entire study reach and also

for the two parts upstream and downstream of the Arc confluence to explore whether there were any clear temporal trajectories of morphological change. The area of the embanked channel under water, exposed bare sediment, and vegetation was calculated using all images that provided near-complete coverage for the full reach and its two parts. These data allowed the proportion of the embanked channel supporting bars (exposed bare sediment plus vegetation), vegetated bars (vegetation), and active bars (exposed bare sediment) to be estimated. In Figure 6 the area of total and vegetated bars is expressed as a proportion of the entire embanked channel area, whereas the area of active bars (bare sediment) is expressed as a proportion of the active channel area (area of exposed bare sediment and water). Despite differences in the temporal distribution of image dates analysed for the whole reach (Figure 6b) and its upstream (Figure 6c) and downstream parts (Figure 6d), all three reaches show clear trajectories of morphological change through the approximately 80 year period analysed. In all cases, the vegetated percentage of the total channel area shows a similar shaped time trajectory, increasing from nearly zero to a near-constant value, which is approximately 35% for the whole reach (Figure 6b), 45% upstream the Arc confluence (Figure 6c) and 25% downstream (Figure 6d). The time interval in which the three trajectories transition between apparently steady states consisting of bare-sediment alternate bars (initial state) and of mostly vegetated alternate bars (present state) is approximately 20 to 30 years. Vegetation encroachment commences in the early 1950s upstream of the Arc confluence and in the 1970s downstream. The detailed time series for the upstream reach also reveals marked temporal fluctuations in vegetation cover, which overlap with the period of most frequent artificial vegetation removal in this part of the river.

Figure 7: Proportion of the embanked channel area that is vegetated in each of the 1 km sections of the study reach extracted from aerial images of different date. The positions of three 3 km sections (subreaches A, B and C) are shown, where a detailed analysis of bar dimensions and migration was undertaken

Morphological evolution was explored in more detail at the scale of 1 km sections, focusing on changes in the vegetated area of the bars (Figure 7). This analysis confirms the early vegetation encroachment in the upstream part of the reach, with negligible vegetation cover in the earliest images; vegetation appearing in km 1 to 4 in the 1950s; penetrating the entire upstream part (km 1 to 13) by the late 1960s; and then progressively occupying a larger area of the embanked channel until the last set of images in 2011. In the downstream part there is early vegetation colonization immediately downstream of the Arc confluence in the 1940s. Thereafter, there is negligible vegetation coverage downstream of the confluence (although note the spatially patchy image coverage) until the mid-1970s when vegetation colonization recommences downstream of the confluence (km 14-21) and starts to propagate upstream from the bottom of the study reach (km 26-33). This broad pattern persists until the 1990s when vegetation cover is evident in all sections (km 14-33) downstream of the confluence. From 1990, vegetation coverage increases but remains lower in the downstream part than upstream, with the highest coverage developing in km 14-16, immediately downstream of the Arc confluence.

Observed morphodynamics of alternate bars with increasing vegetation coverage

Three 3 km subreaches were selected to reflect the broad patterns revealed in Figure 7 and support a more detailed analysis of the bars. These subreaches were located upstream of the Arc confluence (subreach A); a short distance downstream of the confluence (subreach B); and centrally within the downstream part of the study reach (subreach C) (Figure 7).

First, the number of bars, average bar length, and area (total and vegetated) of the embanked channel occupied by exposed bars was calculated for all image dates (Figure 8). Second an analysis was undertaken of the changing position of the centroids of the exposed bars between all image dates, including those with only part coverage of the subreaches (Figure 9). Because of differences in the images available for the subreaches and also the time periods between image dates, the data in Figure 9 can only give an approximate indication of differences in movement rates within and between subreaches. Nevertheless, reliable comparisons can be made across the three subreaches for those images enclosed within black boxes, where the start and end image dates are the same.

Figures 8 and 9 show that the subreaches typically support 5 to 7 bars of 400 to 600 m length which migrate downstream throughout the 80 year period of the analysis. However, there are marked differences in the behaviour of the bars within each of the subreaches and through time, with particularly noticeable shifts in behaviour before and after the late 1970s, and also during the 1950s.

In subreach A, upstream of the Arc confluence, the number of bars remain steady at between 7 and 9 until the late 1970s but with a gradual increase in bar length from

300 to 500 m. This is accompanied by an increase in the channel area occupied by bars from around 35% to over 60%, and, from the mid-1950s, vegetation encroachment from 0% to over 40% cover of the channel area. Throughout the period to the late 1970s, bars migrate downstream slowly and possibly at a decreasing rate (compare the one to two year centroid movements for 1936-7, 1937-39, 1967-68, 1968-69, Figure 9). From the late 1970s to 2011, the number of bars falls dramatically from around 8 to 3, their length more than doubles from approximately 500 m to 1300 m, and they continue to occupy around 50% of the total channel area with vegetation encroaching across virtually the entire exposed bar surfaces. During this time, downstream migration almost ceases (see one year bar centroid movements in 1977-8, 1978-9 and ten year movement between 2001 and 2011, Figure 9), being replaced mainly by bar coalescence.

In subreach B, immediately downstream of the Arc confluence, the number of bars varies between 5 and 8 until the late 1970s with bar lengths of typically 400 m to 600 m and widely varying bar area, occupying between 20% and 60% of the embanked channel. Apart from one image, where the vegetated area is approximately 20%, bars remain largely unvegetated. During this period bars migrate downstream and, based on a comparison of movement of bar centroids in 1968-9 (the only year available for comparison) the rates are faster than those observed in subreach A. From the late 1970s to 2011, there is a slight reduction in the number of bars to between 4 and 5 and a modest increase in average bar length to approximately 800 m accompanied by an increase in the area of the embanked channel occupied by bars (to over 60%) and by vegetated bars (to around 30%). Downstream migration of bars continues at a decreasing rate but faster than in subreach A (compare 1977-8 one year centroid movements, Figure 9) with some apparent recent reversal (2001-

11 ten year movements, Figure 9) that is probably an artifact of bar coalescence and enlargement.

Figure 8: The number, length and area (total and vegetated) of bars within the embanked channel in subreaches A, B and C. Data are drawn from all images providing full coverage of each sub-reach.

Figure 9: The changing position of exposed bar centroids between different start dates (black dots) and end dates (white filled dots). When both the start and end dates are identical for all three subreaches, the subreach maps are enclosed in a box.

In subreach C there is a small increase in the number of bars (4 to 7) until the late 1970s with an initial increase in bar length (from 300 m to 600 m) until the late 1950s followed by a similar decrease by the late 1970s. These changes in average bar length are accompanied by an increase from around 20% to over 50% in the embanked channel area occupied by essentially unvegetated bars in the 1950s followed by a concomitant decrease. During this period bars migrate more rapidly downstream than in subreaches A and B (compare all time periods in the black boxes to 1977-78, Figure 9). From the late 1970s to 2011, the number of bars stabilizes at 6 to 7 with a slight increase in average length to approach 600m, an increase in the channel area occupied by bars from approximately 20% to 50%, and the commencement of vegetation encroachment to around 20% of the channel area by 2011. Bars continue to migrate downstream during this period with no obvious

change in the rate of movement until approximately 2001, after which bar migration almost ceases.

Using the same analysis methods, annual bar centroid movements were estimated for the entire 33 km reach over the period 1936 to 1939, for the years 1968 to 1969 and 1977 to 1978, and over the period 2001-2011 (Figure 10) to assess whether the temporal trends identified for sub-reaches A, B and C were discernible along the entire 33 km reach. In the earliest period (Figure 10a), there was incomplete cover of the 33 km reach, and (based on a short sub-reach where 1937 to 1939 movement could be observed), it appears that most of the bar movement occurred in 1936, so that the plotted averages are far lower than the maximum annual rate was likely to have been at that time. Nevertheless, it appears that from 1936 to 1939 the difference in bar movements between upstream and downstream of the Arc confluence was smaller than the upstream to downstream difference in 1968-9 and 1977-8 (Figure 10 b,c), and the difference was also smaller between 1968 and 1969 than between 1977 and 1978, confirming a more marked temporal reduction in movement rates in sub-reach A (upstream of the confluence) compared to sub-reaches B and C over the time period investigated. The more subtle differences in bar movement rates between sub-reaches B and C are also confirmed by an apparent propagation of the highest rates of movement in a downstream direction from the Arc confluence across the first three analysed dates (Figure 10 a, b, c). Because the aerial image coverage was also incomplete for 1968 to 1969, the persistence in time of the very low movements from kilometre 26 downstream in 1977 to 1978 cannot be established. Lastly, average annual bar movement rates were slowest in all subreaches over the period between 2001 and 2011, indicating a strong general decline in bar movement. For this time period, it was relatively easy to

recognize the same bars from their shapes in most cases, and especially considering that the bars already were in the same place in 1996. However, the 10 year time interval between photographs may have led to some difficulties in relocating the same bars leading to some underestimation of movement rates (Figure 10d).

A further morphological property of alternate bars that is typically correlated with the rate of bar migration is bar wavelength, with migrating bars being shorter compared to steady, non-migrating bars (e.g. Adami et al., 2016). We explored the theoretical behaviour and wavelength of migrating bars at the Isère within a meaningful range of variability of the input parameters of the linear bar theories for both the upstream and downstream subreaches (Table 3). Migrating, free bars are predicted to form under a broad range of discharge conditions, with the channel width to depth ratio β largely exceeding the threshold β_c for free bar instability in both reaches (Table 3). Bar wavelength values have been made dimensionless by scaling them with the reach channel width, to allow comparison among reaches and with rivers of different size. The predicted dimensionless wavelength range of migrating bars fluctuates around 7, which is consistent with observed and theoretically predicted values from earlier studies, that range typically between 6-9 (e.g., Tubino et al., 1999, Adami et al., 2016). Predicted dimensionless wavelengths of steady bars range between 29 and 36. Observed values are plotted in Figure 11 for different years, allowing spatially distributed information on bar migration to be extracted. Before systematic vegetation encroachment (Figure 11a, note the 1948 distribution of percentage vegetation cover across the top of the graph), observed values of dimensionless bar wavelength fall within the predicted range of migrating bars (6 to 9) in almost the entire study reach, with some deviation towards longer values close to the Arc

confluence (vertical short-dashed line) and in the proximity of most of the bends along the reach (vertical long-dashed lines). The bar migration data that can be extracted for this period (1936-1939, Figure 10a) are consistent with the observed wavelength values, with shorter bars tending to migrate, and longer bars tending to be located close to bend and confluence perturbations of the straight channel geometry, where they also tend to be more steady (Struiksma et al., 1985, Tubino et al., 1999). Also the dimensionless bar wavelength values that exceed 10 within km 1 and 2 (Figure 11a) may reflect proximity to a bend located at the upstream end of the study reach. Both observed and predicted wavelengths of steady bars are larger compared to migrating bars, however the wavelengths of steady bars are theoretically overestimated, consistently with Adami et al. (2016).

Figure 10: Annual (average for 1936-1939) downstream migration of exposed bar centroids at three different dates along the 33 km study reach from upstream (left) to downstream (right).

Bar wavelength also shows interesting temporal dynamics. Prior to vegetation establishment (Figure 11a) bar wavelength keeps in the migrating bars range in most of the reach, with higher values systematically observed close to local planform perturbations, namely the 5 bends and the Arc confluence. Between 1977 and 1979 (Figure 11,b), downstream of the Arc confluence there is little to no vegetation development yet between km 15 to 25, and bar wavelengths keep within the range of migrating bars. Between km 25 and 28, where bars were already longer because of the bends, there is evidence of sediment mining in the aerial images in 1977. This

seems to have caused some disturbances which may explain the observed wider spread of wavelength values ranging from 4 to 19. Also near km 4 a human interference is observed on the bars which can be linked to the localized, abrupt increase in bar wavelengths between km 2 and 4. From km 4 to 13 (upstream of the Arc confluence) there is no evidence of human interference in vegetation or sediment removal in these years. Within this reach alternate bars, despite vegetation encroachment, still retain shorter dimensionless wavelengths (< 10, Figure 11b). This reach is of particular interest, showing a very clear response to natural and human disturbances. During 1968 vegetation was removed with excavators (Figure 7 and Figure 3, middle panel) from at least several bars, however it rapidly re-established within a few years (see for example Figure 3, bottom panel). A new attempt to remove vegetation was undertaken in 1972 (Figure 7). Several years later, in 1977, vegetation had encroached again across most of the bar surface (Figure 7 and Figure 8, subreach A). Between 1968 and 1977 the bars probably did not migrated much (Figure 10,b). Furthermore, between October 1977 and September 1978, again very little migration is observed despite a very large migration rate downstream of the Arc confluence (Figure 10,c). The bars seem to be fixed at this time, with vegetation encroachment over most of the bar surface. At the same time, bar wavelengths are seen to increase over a longer timescale of about 20 years (Figure 11,c), showing an initial gradual increase from 1990, with larger values after 2000.

After vegetation establishment, a progressive increase in bar wavelength can be seen in the 1996-2001 time interval over most of the reach (Figure 11c). Bars become consistently longer compared to previous years, particularly in the straight reach just upstream the Arc confluence (km 7 to 13, Figure 11c) and downstream of

kilometre 26. However, between km17 and 26 there are still many shorter wavelengths. This could be linked to the smaller proportion of vegetation encroachment (Figure 7) with less than 50% of the bars covered in reach C (Figure 8, subreach C), where most often the bar tail and/or the bar head are largely unvegetated. Small floods can therefore erode the bare parts including small fractions of the vegetated part, limiting bar elongation. It is possible that vegetation management has taken a role in this process, causing the shorter bar wavelengths in the reaches km 17-26 and km 0-7, however there is no real evidence to confirm this. It should be noted that since 1990's for selected reaches often cutting and/or removal of vegetation for river management purposes was present. Despite cutting and/or removal of vegetation occurred since the 1990s, vegetation has encroached in several reaches over nearly the entire bar surfaces, causing a rapid response in bar migration and a prolonged mode delayed response in bar elongation.

Figure 11: The ratio of bar wavelength to width along the 33km study reach extracted from images captured in (a) 1936, 1937, 1939, 1948 and 1956, (b) 1977, 1978, 1979 and (c) 1996, 2001, 2011. The vegetated proportion of the embanked channel in each 1 km subreach is indicated above each graph and the location of the Arc confluence and major bends in the channel are indicated, respectively, by a short-dashed and long-dashed vertical lines. The grey band on each graph represents the range of bar wavelength/width values expected from bar theory for migrating bars, whereas steady bars would be expected to plot well above the grey band.

Potential controls on channel morphology

Three sets of potentially important human interventions may have impacted upon the biomorphological evolutionary trajectories of the study reach: changes in the river flow regime; mining of riverbed sediment; and the removal of vegetation from bar surfaces.

Flow records were analysed to assess whether any significant changes in river flows could be detected. Four periods of the flow record at Grenoble were analysed: 1905-1928; 1930-1950; 1960-1980; 1996-2016. The average annual patterns of maximum (MAX_QmMEAN), mean (MEAN_QmMEAN), and minimum (MIN_QmMEAN) monthly average flows all show distinct and progressive change over the four time periods (Figure 12), though the most pronounced change seems to occur when the periods before 1950 (Figure 12 a,b,c,d) and after 1960 (Figure 12 e,f,g,h) are compared. Flows in winter increase slightly and flows in summer are greatly reduced, resulting in increasingly subdued seasonal variations in flow that are most noticeable in the MEAN_QmMEAN and MIN_QmMEAN data. The coefficients of variation of monthly flows in the four periods (Figure 12i) also indicate a reduction in flow variability during the winter months through the four time periods. Furthermore, when the 1905-1950/1996-2016 ratios of the monthly MAX_QmMEAN, MIN_QmMEAN and MEAN_QmMEAN values are plotted (Figure 12j) all ratios are higher in the winter than the summer months, with all ratio values exceeding 1.0 between January and April; MIN_QmMEAN and MEAN_QmMEAN ratios exceed 1.0 between October and December; and almost all ratios being less than 1.0 between May and September. These ratios quantify the marked decrease in MAX_QmMEAN and MEAN_QmMEAN values during summer, and a marked decrease in MIN_QmMEAN and MEAN_QmMEAN during winter. This reduction in the range of

monthly flows indicates reduced high flow disturbances and more consistent, reliable low flows, both of which would support vegetation colonization, growth and persistence on bars.

Written records and evidence from aerial images have revealed that sediment mining within the embanked channel (Figure 1) has been concentrated immediately upstream of the study reach, thus affecting sediment delivery to the entire reach. However, sediment mining has occurred within some parts of the study reach, mainly close to Montmélian and to a lesser extent Châteauneuf (Figure 1). Major sediment mining activity was confined to the period 1948-1973 and was discontinued in the mid-1980s (Figure 6).

Vegetation has also been cleared from bar surfaces, in an attempt to control vegetation colonization and stabilization of bars. We used the aerial images (e.g. Figure 3) to identify areas of vegetation clearance at different dates. Clearance usually involves near-surface sediment layers so that the above and below ground components of the vegetation are removed. In Figure 7, the broad within-reach spatial and temporal distribution of major vegetation and accompanying sediment/soil removal activities are superimposed on the pattern of vegetation encroachment so that potential interactions between these processes can be observed. The integrated evidence on vegetation removal indicates that it has been concentrated upstream of the Arc confluence and mainly in the period before capture of the 1977 aerial images. However, since the 1990's (and possibly before), there has been periodic cutting of the vegetation, with in later years complete removal of vegetation including roots and top sediment layers on selected bars. This was not directly observed on the aerial images, probably as a result of the length of the time gaps between images.

Based on the evidence in Figure 7, vegetation and accompanying sediment removal do not seem to be followed by any clear local reduction of vegetation cover in the following years, although these activities may have reduced the rate of expansion of the vegetated area. Furthermore, vegetation recovery following removal is remarkably quick (Figure 3, and some parts of Figure 7), suggesting that removal has only a very temporary effect.

Figure 12: The upper four pairs of graphs (a,b; c,d; e,f; g,h) illustrate the average for each calendar month (MEAN_QmMEAN) of series of mean monthly discharges (QmMEAN – estimated from the daily flow record) observed within four different time periods (1905-1928 (24 years), 1930-1950 (21 years), 1960-1980 (21 years), 1996-2016 (21 years)) and plotted against the maximum average monthly flow (MAX_QmMEAN) in the graphs on the left and the minimum average monthly flow (MIN_QmMEAN) in the graphs on the right. Graph (i) illustrates the coefficient of variation of monthly flows within each month and four time periods and graph (j) illustrates the ratio of the MAX_QmMEAN, MIN_QmMEAN and MEAN_QmMEAN in 1905-1950 to that in 1996-2016.

DISCUSSION

Trajectories of change along the study reach and their likely causes

Analysis of a sequence of air photographs covering approximately a 80 year time period and a 33 km long, channelized and embanked study reach of the River Isère have revealed clear time trajectories of bar development and vegetation encroachment.

Alternate bars characterize the study reach throughout the studied period, but bar density has decreased, bar length has increased, and bar mobility has slowed over time (figures 8, 9, 10). These changes are most marked upstream and gradually decline downstream. They also propagate downstream through the study period (Figures 8, 10) with major changes in bar behaviour discernible before and after the late 1970s. Downstream of the Arc confluence, these major changes correspond with cessation of major bed sediment mining and, especially upstream of the Arc confluence, with most of the evidence of major vegetation and accompanying sediment removal. This also agrees with the results from Vautier et al. (2002) on the Isère river downstream of our study reach, between Pontcharra and Grenoble. Vautier et al. (2002) specified a pre-1970 and post-1970 period: the earlier period characterized by moving bedforms and uprooted pioneer vegetation and the later period showing increased development of vegetation and reduced morphodynamics.

It is also noticeable that the percent channel area occupied by bars in subreaches A, B and C shows a decline from around 1950 (Figure 8), when flow regulation associated with hydropower commenced (Pupier, 1996). This decline persisted to the early 1980's, which marked the end of the period of major gravel mining and most vegetation clearance and the commencement of the installation of sediment weirs (Peiry et al., 1994). Thus a reduction in bar area between approximately 1950 and 1980 appears to be associated with the combined effects of a changed flow regime, a reduced sediment supply from upstream, and major removal of sediment (and vegetation) and the creation of associated gravel pits that could destabilize the bed and sediment movement within the study reach.

Vegetation colonization and encroachment across bar surfaces accompanied these temporal changes in bar density, size and mobility. Upstream of the Arc confluence,

vegetation colonization commenced in the late 1940s (Figure 7), accompanying major changes in the flow regime as the hydropower scheme was implemented from the early 1950s. The Isère-Arc diversion also strongly affected this upstream part and was implemented at about the same time. Since the early 1950s, vegetation encroachment has steadily progressed upstream, typically reaching 50% channel area and 90% bar coverage in recent years (e.g. Figure 8, subreach A). Downstream, early encroachment was patchy and short-lived, with progressive encroachment delayed until the mid-1970s. Since then, encroachments have been progressive, currently reaching around 20-30% channel area and 50% bar coverage (e.g. Figure 8, subreaches B and C).

Before 1950, the relatively undisturbed flow and sediment transport regimes would have caused permanent rejuvenation of bedforms through bar migration and elimination of pioneer plant succession (Girel et al., 2003). Although reduced disturbance and more reliable low flows from the early 1950s are undoubtedly a major influence on vegetation encroachment, fluctuations in vegetation cover between approximately 1950 and 1980 most likely also reflect a reduced sediment supply from upstream and associated sediment removal within the study reach. Furthermore, the integrated changes in flow and sediment transport regimes and sediment availability attributable to the combined effects of hydropower development, sediment mining, and vegetation removal, may well have resulted in river bed incision, increasing the elevation of vegetated bar areas relative to flow disturbances but also increasing the elevation of established vegetation above likely water table levels within the bars, as observed by Dufour et al. (2007) on the Drôme river, France. Installation of sediment weirs since the 1980s may be helping to

control this incision and regulate sediment movement, but are unlikely to have reversed these problems.

Such complex potential adjustments along the study reach require further research, but observations from other rivers (e.g. the River Tagliamento in NE Italy, Gurnell, 2016, Surian et al., 2015) illustrate critical interactions between flow disturbances, groundwater availability, and vegetation growth performance, which in turn affect the ability of colonizing vegetation to stabilize and retain bar sediments and so affect bar size, morphology, and stability. Recent research (Holloway et al, 2017, a,b,c) has illustrated the considerable rooting depth of one widespread riparian tree species (*Populus nigra*); that root profiles can show greater density at depth in relatively drier locations; and that flow disturbances that damage but do not remove riparian trees result in extremely complex subterranean shoot and root profiles. All of these properties of the underground biomass of some riparian trees have the potential to retain and stabilize bar sediments once trees become established and indicate why biomorphological interactions on gravel bars are probably critical to bar density, size, and mobility. In addition, the deep rooting and potential resprouting of such riparian tree species may explain why, after apparent complete removal of vegetation cover, there is such rapid recovery of vegetation across bar surfaces (Figure 3). Allain-Jegou (2002) confirms the importance of roots to bar stabilization in the Isère River by limiting erosion processes. The study further reveals that small floods mainly have the effect of increasing fine sediment deposition on the bars thus favouring both bar aggradation and vegetation growth. Information from field visits and published sources (Allain-Jegou, 2002; Girel, 2003) indicate a decline of biodiversity despite a growth in vegetation area, as pioneer species disappear and more homogeneous hardwood species replace them. Previous research has also linked gravel mining to

locally severe bed incision (Peiry et al., 1994; Vautier, 2000) leading to bed and sediment transport instability.

Further research is underway on the three-dimensional form of the study reach and its association with above-ground vegetation biomass in order to further understand the response of bars to vegetation development and any channel bed incision and long profile changes within the study reach. An integrated approach between analytical and numerical modelling and observations from field and remotely-sensed data is needed to allow a closer connection to be made between the morphological evolution of the reach and possible controlling factors. This can also take advantage of recent developments in modelling approaches for river biomorphodynamics (e.g. Bertoldi et al., 2014) in order to isolate effects of process changes.

The shift from bare sediment to vegetated alternate bars

The unvegetated morphodynamics of the impressively regular sequence of alternate bars that have developed in the Isère following channelization is consistent with previous theoretical morphodynamic work (Tubino et al., 1999, Zolezzi and Seminara, 2001) and with the few existing field observations on analogous cases (Adami et al., 2016). Shorter bars, in the dimensionless bar wavelength range 6 to 9 (normalized using the local, sub-reach averaged channel width), characterized most of the straight sub-reaches of the study area, which can theoretically promote the development of migrating ‘free’ bars of comparable length. For the few years and sub-reaches in which it was possible to reliably compute rates of alternate bar migration (Figure 10a) it appears that these short bars migrated in the straight reaches, while they did not migrate near the local persistent perturbations of channel

geometry, such as the Arc confluence or gently curved river bends. Close to these features, our analysis shows, almost invariably, a local reduction of bar migration rates (Figure 10, all panels) and often a local increase in bar wavelength. Such behaviour is also in close agreement with morphodynamic theories and further confirms the findings of Adami et al. (2016) on the Alpine Rhine River.

Figure 13: Images of subreach A in 1939 and 2014, subreach C in 1948 and 2014, and a similar length section of the embanked River Rhine in 2014 (source images 1939 and 1948: Institut Géographique National; source images 2014: Esri, DigitalGlobe, GeoEye, Earthstar Geographics, CNES/Airbus DS, USDA, USGS, AEX, Getmapping, Aerogrid, IGN, IGP, swisstopo, and the GIS User Community)

Comparison of bar wavelength and migration over time and along the whole study reach (Figures 10 and 11), together with the comparison between morphodynamic theories and observations, suggest an overall slowing effect of vegetation on the migration of alternate bars and a tendency to promote their elongation. The good agreement between predicted bar length and migration properties with those observed prior to systematic vegetation encroachment indeed suggest that the widespread presence of shorter migrating bars in most of the straight reaches represents a morphodynamic equilibrium in the absence of vegetation (which is not accounted for in morphodynamic theories). Longer nonmigrating bars observed only close to bends and to the confluence can for the same reason be attributed to the presence of these local geometrical discontinuities in the channel planform. Cessation of migration and further elongation, which was observed after the

commencement of flow regime regulation, can therefore be related to the accompanying process of systematic vegetation development. The analysis of aerial images suggests that these two effects may act on different timescales, with migration ceasing quite rapidly (in a few years) during vegetation establishment and bar elongation occurring over longer timescales (one or more decades) following processes of sediment deposition upstream and downstream of the vegetated portion of the alternate bar, leading in some cases to bar coalescence (e.g. Figure 13). The image analysis indicates that at a certain time (which depends on the specific location in the reach), the river was no longer able to remove pioneer vegetation and so vegetation continued growing. Once vegetation occupied a large enough proportion of the bar area, no further bar migration could be detected. Bar migration indeed requires sediment deposition to occur at the bar head and, at the same time, the tail of the bar needs to be partially eroded. The latter becomes severely hampered once the bar is mostly vegetated. Bar elongation is observed where bars are nearly completely covered with vegetation. Indeed gravel sediment transport is not stopped by vegetation encroachment and newly deposited gravel patches in between nearby bars on the same bank can be rapidly colonized thus promoting bar coalescence and thus elongation.

The exact timing of these processes is difficult to extract from the images because: the images are often quite widely spaced in time; images of the early stages of vegetation colonization are relatively rare; and during the entire study period there was quite widespread human removal of vegetation. However, the cessation of bar migration and the growth of vegetation are intertwined, as confirmed by Allain-Jegou (2002), who describes vegetation expanding, trapping, and stabilizing sediments as the plant roots form a framework limiting erosion.

The evolution of the Isère River from a totally bare-sediment, alternate bar river system into a heavily vegetated one contrasts with the contemporary evolution of other embanked, regulated river systems such as the Alpine Rhine (see illustration at the bottom of Figure 13), which is located in an analogous geographic setting (bottom of an Alpine valley), had a similar pre-channelization planform morphology (braided – wandering), and has an analogous history of human stressors (gravel mining, complex hydropower regulation, vegetation clearance). While an analogous long-term historical study of the morphological trajectories for the Alpine Rhine has yet to be published, other research (Jäggi, 1984, Adami et al., 2016) suggests that the alternate bars that have developed in a 40 km reach of the Alpine Rhine have reached a rather stable, dynamic equilibrium characterized by longer, steady bars in its upstream part and shorter, migrating bars downstream, with negligible or very limited vegetation development. Such a state is qualitatively comparable to the pre-regulated condition of the Isère, and in both systems it seems to have persisted as a morphodynamic equilibrium for many decades. In contrast, the biomorphological spatial and temporal trajectories identified for the study reach on the Isère River (Figures 6 and 7) suggest that once vegetation has started to colonize bars, it can spread through an entire, homogeneous subreach within approximately 20-30 years. While the Isère may have reached an analogous dynamic equilibrium configuration of bare sediment alternate bars prior to 1950 (Figure 13a), its whole 80 km alternate bar reach (including our study area and the reach analysed by Vautier et al., 2002) has clearly shifted towards a markedly different, less dynamic equilibrium state. This evolutionary trajectory could not be counteracted by vegetation clearance once it had started, as witnessed by the rapid recovery of vegetation following clearance (Figure 3). Interestingly, the shape of the trajectory (Figure 6) of unvegetated-vegetated bar

development resembles the functional shape of the temporal evolution of the amplitude of free bars from an initial exponential growth (linear instability) followed by a nonlinear damping, before asymptotically tending towards an equilibrium value (Colombini et al., 1987). Such similarity suggests that at some stage the alternate bar system in the Isère may have been subject to another instability mechanism which has caused a pronounced shift towards a markedly different vegetated condition. Similar trajectories of vegetation encroachment related to a variety of human impacts have been described in other river systems with different morphologies (e.g. Tal et al., 2004; David et al., 2016; Liébault and Piégay, 2002).

In the light of this, at least two future research developments are suggested by the present analysis. The triggering dynamics of vegetation colonization need to be investigated, and an approach to their further development (in contrast to other systems like the Alpine Rhine) should be explored and based on complex biophysical instability processes, possibly using recently proposed frameworks (e.g. Bertagni et al., 2017) and also including the role of fine suspended sediment transport, which is known to have played a key role in the vertical development of the vegetated bars in the Isère (Allain-Jegou et al., 2002). If instability is confirmed to be relevant to this problem, a second development should be explored, emphasizing the possible effect of riparian vegetation on the morphodynamics of alternate bars. However, given the relevance of initial conditions on instability mechanisms, further work should focus on related feedback effects, that is how the morphodynamics of bare-sediment alternate bars may have affected vegetation development.

Limitations to the analysis

Despite having successfully recognized some clear trajectories of change along the studied reach of the River Isère and having interpreted these in the context of both theory and likely causal factors, it is important to stress some limitations of our analysis.

Dependence upon historical records has constrained the temporal resolution and spatial extent of our analyses. This is a particularly important limitation when abrupt changes in aerial image cover occur between the points in time for which data are available and in the locations of extended spatial data gaps, since interruptions in time and space may disguise important changes that cannot be characterized. Nevertheless, the availability of aerial images has been generally good in the present study, and the prolonged flow record has been very helpful in characterizing changes and exploring their potential causes. Available information on sediment mining was also quite extensive, with a reasonable indication of where, when and how much sediment was removed from the study reach. However, information on vegetation clearance from bar surfaces depended upon interpretation of aerial images and, given the rapid rate of recovery of vegetation following clearance (e.g. Figure 3), our data on the location, extent and timing of vegetation clearance is very likely to be an underestimate.

A further limitation is the varying spatial resolution and geometry of the analysed images. We undertook a positional error analysis following geocorrection and georeferencing of the images, which has given reassuring results, but it is difficult to assess the impact of image resolution and whether images are colour or panchromatic on the identification and accurate digitizing of features of interest.

CONCLUSIONS

We have investigated the multidecadal (80 years) biomorphodynamics of alternate bars in a 33 km reach of the channelized and regulated Isère River in SE France, a remarkable case of complex morphological response to the effects of multiple human interventions. We have employed a combination of historical image processing, analysis of flow records and historical documents, and the application of morphodynamics analytical theories to quantify such evolution and discuss how multiple human interventions might have affected them. Alternate bars consisting of bare sediment likely appeared soon after channelization in the mid-1800s and have characterized the study reach mainly in the form of migrating bars, with length and migration properties consistent with analytical theories and observations on channelized rivers with similar responses. After the beginning of major hydropower development and sediment mining from the early 1950s, vegetation progressively encroached across the exposed bar surfaces showing similar evolutionary trajectories in parts of the river located upstream and downstream of the major confluence with the Arc River. Thus, the system first evolved towards an equilibrium configuration of mainly bare, migrating alternate bars and then towards a different, less dynamic equilibrium configuration characterized by longer, mostly non-migrating, vegetated bars. These evolutionary trajectories correspond qualitatively to alterations in the monthly flow regime. However, vegetation encroachment started approximately 20 years earlier in the upstream part of the reach, which is more strongly affected by a major flow diversion, and where most sediment mining is documented. Human clearance of vegetation only seems to be able to perturb the new equilibrium state temporarily.

Future analysis of historical information for the Isère River will concentrate on the vertical responses of the channel morphology that accompanied the observed planform changes. However, the outcomes of the present analysis offer an interesting benchmark for the development and application of novel theoretical and modelling approaches needed to formulate and verify biophysically-based hypotheses to explain the system shift between two markedly different equilibrium states. Such work can also be developed in relation to evidence emerging from other channelized and regulated Alpine rivers with alternate bars where such a biophysical shift has not yet occurred. Besides gaining more insight into the functioning of these specific river systems, integration of modelling and observational approaches on such benchmark cases has a strong potential to reveal yet poorly understood biophysical interactions affecting a broader class of gravel bed rivers.

ACKNOWLEDGEMENTS

Alyssa Serlet's research is funded by the SMART Joint Doctoral Programme (Science for MAnagement of Rivers and their Tidal systems), which is financed by the Erasmus Mundus Programme of the European Union. The sources of the historical data used in this research are all fully cited in tables or within the text. We would like to thank Électricité de France (EDF) and the Syndicat Mixte de l'Isère et de l'Arc en Combe de Savoie (SISARC) for their support. We also thank the Isère Departmental Archives and support of Denis Coeur to collect the historical documents.

REFERENCES

Abate M, Nyssen J, Steenhuis TS, Moges MM, Tilahun SA, Enku T, Adgo E. 2015. Morphological changes of Gumara River channel over 50 years, upper Blue Nile basin, Ethiopia. Journal of Hydrology 525: 152–164.

Adami L, Bertoldi W, Zolezzi G. 2016. Multidecadal dynamics of alternate bars in the Alpine Rhine River. Water Resources Research 52: 8938–8955.

Alcayaga H. 2013. Impacts morphologiques des aménagements hydroélectriques à l'échelle du bassin versant (PhD thesis). Université de Grenoble.

Allain-Jegou C. 2002. Rélations végétation - écoulement - transport solide dans le lit des rivières. étude de l'Isère dans le Grésivaudan (PhD thesis). Institut National Polytechnique de Grenoble

Asaeda T, Rashid MH. 2012. The impacts of sediment released from dams on downstream sediment bar vegetation. Journal of Hydrology 430–431: 25-38.

Badel A-C. 2000. Modélisation des crues historiques de la moyenne Isère.

Belletti B, Nardi L, Rinaldi M. 2016. Diagnosing problems induced by past gravel mining and other disturbances in Southern European rivers: the Magra River, Italy. Aquatic Sciences 78(1): 107-119.

Bertagni M, Perona P, Camporeale C. 2017. Floquet theory of river ecomorphodynamics Geophysical Research Abstracts 19, EGU2017-15347

Bertoldi W, Siviglia A, Tettamanti S, Toffolon M, Vetsch D, Francalanci S. 2014. Modeling vegetation controls on fluvial morphological trajectories. Geophysical Research Letters 41(20): 7167-7175.

Bravard J-P. 1989. La metamorphose des rivières des alpes françaises à la fin du moyen-âge et à l'époque moderne. Bulletin de la Société Géographique de Liège 25: 145–157

Brierley G, Fryirs K. 2005. Geomorphology and River Management: Applications of the River Styles Framework. Blackwell Publishing, Malden, MA, USA.

Camporeale C, Perucca E, Ridolfi L, Gurnell AM. 2013. Modeling the interactions between river morphodynamics and riparian vegetation. Reviews of Geophysics 51(3): 379-414.

Choi SU, Yoon B, Woo H. 2005. Effects of dam-induced flow regime change on downstream river morphology and vegetation cover in the Hwang River, Korea. River Research and Applications 21 (2–3): 315–325. DOI:10.1002/rra.849.

Clément M. 2011. L'endiguement de l'Isère et de l'Arc - études & travaux au XIXe siècle. Association des Amis de Montmélian et de ses Environs (ed.).

Clerici A, Perego S, Chelli A, Tellini C. 2015. Morphological changes of the floodplain reach of the Taro River (Northern Italy) in the last two centuries. Journal of Hydrology 527: 1106–1122.

Colombini M, Seminara G, Tubino M. 1987. Finite-amplitude alternate bars. Journal of Fluid Mechanics 181 (9): 213–232. DOI:10.1017/S0022112087002064.

Comiti F, Da Canal M, Surian N, Mao L, Picco L, Lenzi MA. 2011. Channel adjustments and vegetation cover dynamics in a large gravel bed river over the last 200 years. Geomorphology 125(1): 147-159.

Corenblit D, Steiger J, Charrier G, Darrozes J, Garófano-Gómez V, Garreau A, González E, Gurnell AM, Hortobágyi B, Julien F, Lambs L, Larrue S, Otto T, Roussel E, Vautier F, Voldoire O. 2016. Populus nigra L. establishment and fluvial landform

construction: biogeomorphic dynamics within a channelized river. Earth Surface Processes and Landforms 41(9): 1276-1292.

David M, Labenne A, Carozza JM, Valette P. 2016. Evolutionary trajectory of channel planforms in the middle Garonne River (Toulouse, SW France) over a 130-year period: Contribution of mixed multiple factor analysis (MFAmix). Geomorphology 258, Elsevier B.V., 21–39. DOI:10.1016/j.geomorph.2016.01.012.

Didier M. 1994. Relation entre l'enfoncement du lit de l'Isère et la stabilité de ses îles dans le Grésivaudan. Revue de Géographie Alpine 2: 147–155.

Dufour S, Barsoum N, Muller E, Piégay H. 2007. Effects of channel confinement on pioneer woody vegetatiojn structure, composition and diversity along the River Drôme (SE France). Earth Surface Processes and Landforms 32: 1244-1256.

Fryirs K, Spink A, Brierley G. 2009. Post-European settlement response gradients of river sensitivity and recovery across the upper Hunter catchment, Australia. Earth Surface Processes and Landforms 34: 897-918.

Garcia Lugo GA, Bertoldi W, Henshaw AJ, Gurnell AM. 2015. The effect of lateral confinement on gravel bed river morphology. Water Resources Research 51, 7145–7158. DOI:10.1002/ 2015WR017081.

Girel J, Vautier F, Peiry J. 2003. Biodiversity and land use history of the alpine riparian landscapes (the example of the Isère river valley, France). Multifunctional Landscapes, 3: 167–200.

Girel J. 2010. Histoire de l'endiguement de l'Isère en Savoie: conséquences sur l'organisation du paysage et la biodiversité actuelle. Géocarrefour 85 (1): 41–55.

González del Tánago M, Martínez-Fernández V, García de Jalón D. 2016. Diagnosing problems produced by flow regulation and other disturbances in

Southern European Rivers: the Porma and Curueno Rivers (Duero Basin, NW Spain). Aquatic Sciences 78: 121-133.

Grabowski RC, Gurnell AM. 2016. Using Historical Data in Fluvial Geomorphology. In: Kondolf GM, Piégay H (eds). Tools in Fluvial Geomorphology, 2nd ed, John Wiley & Sons, Ltd; 56–75.

Grabowski RC, Surian N, Gurnell AM. 2014. Characterizing geomorphological change to support sustainable river restoration and management. WIREs Water 2014, DOI: 10.1002/wat2.1037.

Gurnell AM. 2016. Trees, wood and river morphodynamics: results from 15 years research on the Tagliamento river, Italy. In Gilvear DJ, Greenwood MT, Thoms MC, Wood PJ (eds). River Science: Research and Applications for the 21st Century; 132-155, John Wiley and Sons Ltd., Chichester, UK, DOI: 10.1002/9781118643525.ch7.

Gurnell AM, Rinaldi M, Belletti B, Bizzi S, Blamauer B, Braca G, Buijse AD, Bussettini M, Camenen B, Comiti F, Demarchi L, García de Jalón D, González del Tánago M, Grabowski RC, Gunn IDM, Habersack H, Hendriks D, Henshaw AJ, Klösch M, Lastoria B, Latapie A, Marcinkowski P, Martínez-Fernández V, Mosselman E, Mountford JO, Nardi L, Okruszko T, O'Hare MT, Palma M, Percopo C, Surian N, van de Bund W, Weissteiner C, Ziliani L. 2016. A multi-scale hierarchical framework for developing understanding of river behaviour to support river management. Aquatic Sciences 78(1): 1-16.

Holloway JV, Rillig MC, Gurnell AM. 2017a. Underground Riparian Wood: Buried Stem and Coarse Root Structures of Black Poplar (Populus nigra L.). Geomorphology 279: 188-198.

Holloway JV, Rillig MC, Gurnell AM. 2017b. Underground Riparian Wood: Reconstructing the Processes Influencing Buried Stem and Coarse Root Structures of Black Poplar (Populus nigra L.). Geomorphology 279: 199-208.

Holloway JV, Rillig MC, Gurnell AM. 2017c. Physical Environmental Controls on Riparian Root Profiles associated with Black Poplar (Populus Nigra L.) along the Tagliamento River, Italy. Earth Surface Processes and Landforms. DOI: 10.1002/esp.4076

Institut National de l'Information Géographique et Forestière. (n.d.). Géoportail. [Online]. Available at: https://remonterletemps.ign.fr [Accessed: 22 December 2016].

Jaballah M, Camenen B, Pénard L, Paquier A. 2015. Alternate bar development in an alpine river following engineering works. Advances in Water Resources 81: 103-113.

Jäggi M. 1984. Formation and effects of alternate bars, Journal of Hydraulic Engineering, 110(2): 142–156. DOI:10.1061/(ASCE)0733-9429(1984)110:2(142).

Jourdain C. 2017. Action des crues sur la dynamique sédimentaire et végétale d'un lit de rivière à galets: l'Isère en Combe de Savoie (PhD thesis), Université Grenoble Alpes

Kiss T, Blanka V. 2012. River channel response to climate- and human-induced hydrological changes: Case study on the meandering Hernád River, Hungary. Geomorphology 175-176: 115-125.

Lang M, Coeur D, Brochet S, Naudet R. 2003. Information historique et ingénierie des risques naturels. L'Isère et le torrent du Manival. Cemagref Editions, série Gestion des milieux aquatiques.

Lanzoni S. 2000. Experiments on bar formation in a straight flume: 2. graded sediment, Water Resources Research 36(11): 3351–3363. DOI: 10.1029/2000WR900161.

Liébault F, Piégay H. 2002. Causes of 20th century channel narrowing in mountain and piedmont rivers of Southeastern France. Earth Surface Processes and Landforms 27(4): 425-444.

Meyer-Peter E, Müller R. 1948. Formulas for bedload transport. In Second meeting, international association of hydraulic engineering and research, Stockholm.

Magliulo P, Bozzi F, Pignone M. 2016. Assessing the planform changes of the Tammaro River (southern Italy) from 1870 to 1955 using a GIS-aided historical map analysis. Environmental Earth Sciences 75(355): 1-19.

Molnar, P., Favre, V., Perona, P., Burlando, P., Ruf, W. 2008. Floodplain forest dynamics in a hydrologically altered mountain river. Peckiana, Staatliches Museum für Naturkunde Görlitz, 5:17-24

Pasquale, N., Perona, P., Schneider, P., Shrestha, J., Wombacher, A., Burlando, P. 2011. Modern comprehensive approach to monitor the morphodynamic evolution of a restored river corridor, Hydrol. Earth Syst. Sci., 15, 1197-1212, https://doi.org/10.5194/hess-15-1197-2011

Peiry J, Salvador P, Nouguier F. 1994. L' incision des rivières dans les Alpes du nord : état de la question / River incision in the Northern French Alps. Revue de géographie de Lyon 69 (1): 47–56. DOI:10.3406/geoca.1994.4237.

Petts GE. 1989. Historical Analysis of Fluvial Hydrostystems. In: Petts, G. E., Moller, H. and Roux, A. L. (eds.), Historical change of large alluvial rivers. Western Europe., John Wiley & Sons Ltd; 1–18.

Provansal M, Dufour S, Sabatier F, Anthony EJ, Raccasi G, Robresco S. 2014. The geomorphic evolution and sediment balance of the lower Rhone River (southern France) over the last 130years: Hydropower dams versus other control factors. Geomorphology 219: 27-41.

Pupier N. 1996. Analyse des fluctuations récentes de la nappe d'un hydrosystème perturbé, l'Isère dans le Grésivaudan (PhD thesis). Institut de Géographie Alpine. Université Joseph Fourier, Grenoble.

Rinaldi M, Wyzga B, Surian N. 2005. Sediment mining in alluvial channels: Physical effects and management perspectives. River Research and Applications 21(7): 805-828.

Rinaldi M, Bussettini M, Surian N, Comiti F. 2011. Analisi e valutazione degli aspetti idromorfologici. ISPRA - Istituto Superiore per la Protezione e la Ricerca Ambientale - Rome, Italy ISBN: 9788844804398, 85p (in Italian)

Ritter J. 1959. L' aménagement hydroélectrique du bassin de l' Isère. Annales de Géographie 69 (365), 34–53.

Rodrigues S, Mosselman E, Claude N, Wintenberger CL, Juge, P. 2015, Alternate bars in a sandy gravel bed river: generation, migration and interactions with superimposed dunes, Earth Surface Processes and Landforms 40(5): 610–628. DOI:10.1002/esp.3657.

Schirmer, M., Luster, J., Linde, N., Perona, P., Mitchell, E. A. D., Barry, D. A., Hollender, J., Cirpka, O. A., Schneider, P., Vogt, T., Radny, D., Durisch-Kaiser, E. 2014. Morphological, hydrological, biogeochemical and ecological changes and challenges in river restoration – the Thur River case study, Hydrol. Earth Syst. Sci., 18, 2449-2462, https://doi.org/10.5194/hess-18-2449-2014

Scorpio, V., Zen, S., Bertoldi, W., Surian, N., Mastronunzio, M., Dai Prá, E., Zolezzi, G. Comiti, F. 2018. Channelization of a large alpine river: what is left of its original morphodynamics? Earth Surface Processes and Landforms, in press.

Seminara G, Tubino M. 1992. Weakly nonlinear theory of regular meanders. Journal of Fluid Mechanics 244 (11): 257–288. DOI:10.1017/S0022112092003069.

Siviglia A, Repetto R, Zolezzi G, Tubino M. 2008. River bed evolution due to channel expansion: general behaviour and application to a case study (Kugart River, Kyrgyz Republic). River Research and Applications 24: 1271-1287.

Stäuble S, Martin S, Reynard E. 2008. Historical mapping for landscape reconstruction: examples from the Canton of Valais (Switzerland). In: Mountain Mapping and Visualisation, Proceedings of the 6th ICA Mountain Cartography Workshop 11–15 February 2008, Lenk, Switzerland; 211–217

Struiksma N, Olesen KW, Flokstra C, De Vriend HJ. 1985. Bed deformation in curved alluvial channels. Journal of Hydraulic Research 23 (1): 57–79. DOI:10.1080/00221688509499377.

Surian N, Barban M, Ziliani L, Monegato G, Bertoldi W, Comiti F. 2015. Vegetation turnover in a braided river: frequency and effectiveness of floods of different magnitude. Earth Surface Processes and Landforms 40: 542–558. DOI:10.1002/esp.3660.

Tal M, Gran K, Murray AB, Paola C, Hicks DM. 2004. Riparian vegetation as a primary control on channel characteristics in multi-thread rivers. In: Bennett, S. J. and Simon, A. (eds.), Riparian vegetation and fluvial geomorphology, Washington, DC: American Geophysical Union. DOI:10.1029/008WSA04.

Tealdi S, Camporeale C, Ridolfi L. 2011. Long-term morphological river response to hydrological changes. Advances in Water Resources 34(12): 1643–1655.

Tubino M, Repetto R, Zolezzi G. 1999. Free bars in rivers, Journal of Hydraulic Research 37(6): 759–775. DOI:10.1080/00221689909498510.

Urban MA, Rhoads BL. 2003. Catastrophic Human-Induced Change in Stream-Channel Planform and Geometry in an Agricultural Watershed, Illinois, USA. Annals of the Association of American Geographers 93(4): 783-796.

Vautier F. 2000. Dynamique geomorphologique et végétalisation des cours d'eau endigues: l'exemple de l'Isère dans le Grésivaudan (PhD thesis). Institut de Géographie Alpine, Université Joseph Fourier, Grenoble.

Vautier F, Peiry J-L, Girel J. 2002. Dévéloppement végétal dans le lit endigué de l'Isère en amont de Grenoble: du dianostic à l'évaluation des pratiques de gestion. Revue d'Ecologie (La Terre et la Vie) 57 (2): 65–79.

Vivian H. 1969. Les crues de l ' Isère à Grenoble et l ' aménagement actuel des digues. Revue de géographie alpine 57 (1): 53–84.

Woelfle-Erskine C, Wilcox AC, Moore JN. 2012. Combining historical and process perspectives to infer ranges of geomorphic variability and inform river restoration in a wandering gravel-bed river. Earth Surface Processes and Landforms 37(12): 1302-1312.

Zanoni L, Gurnell A, Drake N, Surian N. 2008. Island dynamics in a braided river from analysis of historical maps and air photographs. River Research and Applications 24(8): 1141-1159.

Zen S, Zolezzi G, Toffolon M, Gurnell AM. 2016. Biomorphodynamic modelling of inner bank advance in migrating meander bends. Advances in Water Resources 93: 166-181.

Zolezzi G, Seminara G. 2001. Downstream and upstream influence in river meandering. part 2. planimetric development, Journal of Fluid Mechanics 438: 183–211. DOI:10.1017/S002211200100427X.

Zolezzi G, Bertoldi W, Tubino M. 2012. Modelling Morphodynamics Morphodynamics of Bars in Gravel-bed Rivers : Bridging Analytical Models and Field Observations. In: M. Church, P. Biron and A. Roy (Eds), Gravel-Bed Rivers: Processes, Tools, Environments. Wiley-Blackwell; 69-89.

Table 1: Hydrological information on the river basin upstream of the Arc confluence at Albertville, downstream the confluence at Montmélian and further downstream in Grenoble

	Upstream of the Arc confluence (Albertville)	**Downtream of the Arc confluence (Montmélian)**	**Grenoble**
Size of water basin* (not taking into consideration flow diversions)	2576 km²*	4703 km²*	5817 km²*
Mean discharge	53 m^3s^{-1}**	121 m^3s^{-1}***	178 m^3s^{-1}
2 year return period daily discharge	Not Available	360 m^3s^{-1}***	500 m^3s^{-1}***

Sources: *(Alcayaga, 2013); **(Jourdain, 2017); ***(Banque Hydro)

Table 2: Dates, study reach coverage (in km from 1 (upstream) to 33 (downstream) along the study reach) and approximate spatial scale of the aerial images analysed, accompanied when available by the daily discharge monitored at Grenoble for the image date. (Note that precise dates are not available for all images, preventing the concurrent daily discharge from being estimated).

Date of image capture	**Image coverage (1 km sections of the study reach)**	**Approximate spatial scale**	**Estimated daily discharge [m^3s^{-1}]**
??/04/1931	16-19	1/10800	-
25/05/1936	10-22	1/18800	317
??/??/1937	1-12	1/29000	-
??/07/1939	1-6;	1/21500	-
??/07/1939	23-33	1/21500	-
??/08/1939	6-23	1/29000	-
25/08/1948	1-3	1/41000	263
26/08/1948	27-33	1/37500	259
4/10/1948	4-30	1/23000	120
18/07/1956	11-14	1/28000	204
26/07/1956	15-22	1/28000	158
26/07/1956	31-33	1/31500	158
13/08/1956	1-10	1/28000	-
13/08/1956	23-30	1/33300	-
11/06/1964	17-23	1/27500	147
11/10/1967	1-14	1/31700	109

??/??/1968	1-14	1/20000	-
??/??/1968	15-28	1/31000	-
12/09/1969	1-22	1/23500	118
??/??/1970	13-29	1/21200	-
1/06/1970	29-33	1/17000	416
10/08/1972	1-33	1/16000	102
2/10/1975	19-33	1/29000	157
19/10/1977	1-31	1/23000	125
16/09/1978	17-33	1/30000	154
24/09/1978	1-17	1/29000	113
18/07/1979	1-22	1/60000	187
14/08/1980	13-33	1/62000	244
8/07/1982	1-33	1/15000	345
12/08/1982	1-19	1/27000	182
7/07/1984	17-26	1/29500	-
20/08/1987	1-24	1/29000	201
21/07/1990	21-33	1/22000	158
22/07/1990	1-21	1/24000	125
1/08/1996	24-29	1/28000	137
17/08/1996	7-23	1/35000	93
18/08/1996	1-6	1/33000	80
18/08/1996	30-33	1/31000	94
22/07/2001	1-33	1/31000	216
10/06/2011	1-33	-	180

Table 3

Reach	Input values range				Output values range			
	W (m)	Q ($m^3.s^{-1}$)	S (%)	D_{50} (mm)	β	β_{cr}	$(L/W)_{migrating}$	$(L/W)_{steady}$
Upstream	90-110	105-285	0.17-0.23	19-28	32.3-47.3	4.8-8.2	6.9-7.7	29.4-36.1
Downstream	115-135	360-490	0.13-0.22	17-28	33.7-43.6	6.6-9.5	6.9-7.1	29.5-31.5

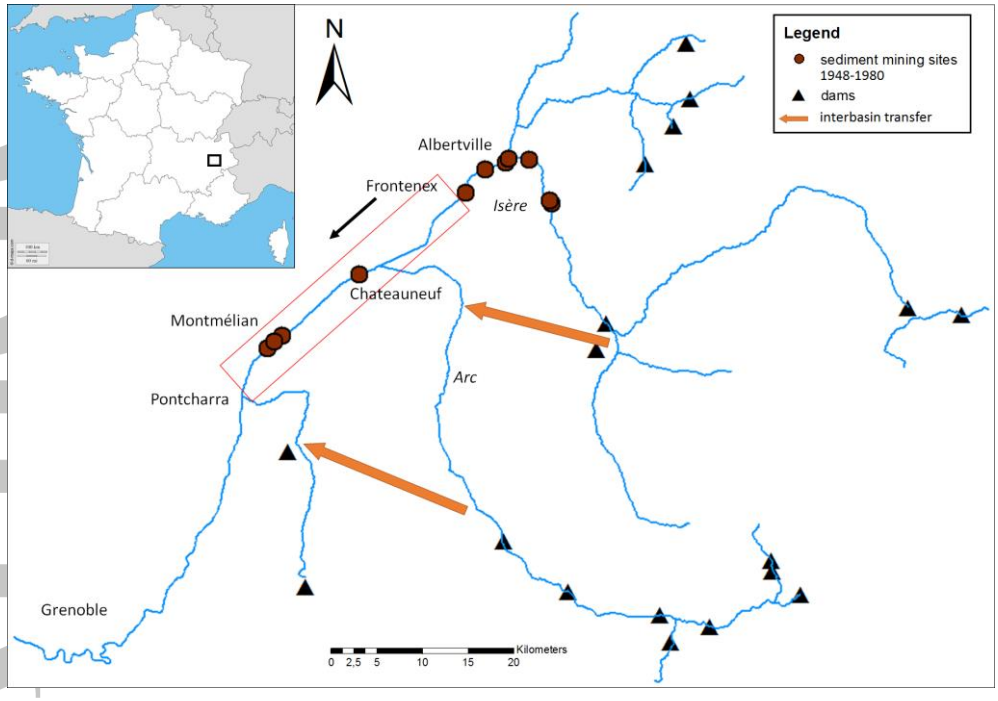

Figure 1: The location of the study reach of the River Isère showing the locations of major dams, interbasin transfers and sediment mining in and upstream of the study reach (where > 20000 m^3 of sediment were extracted during the mid-20th century).

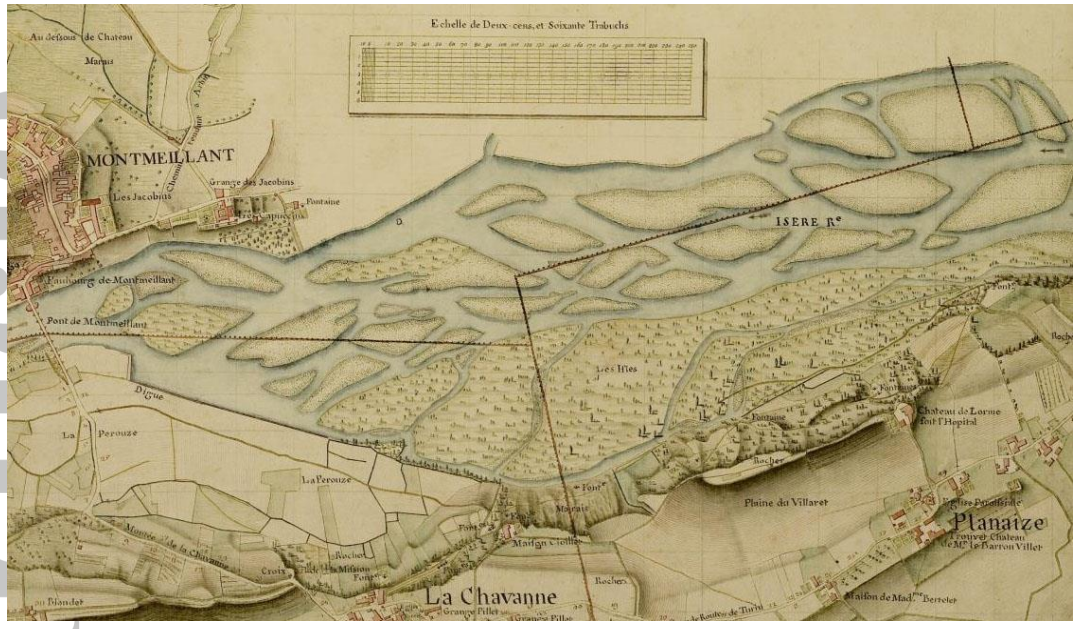

Figure 2: The River Isère near Montmélian in 1781-2, before channelization (source: the Marchetti map, Archives Départementales de la Savoie)

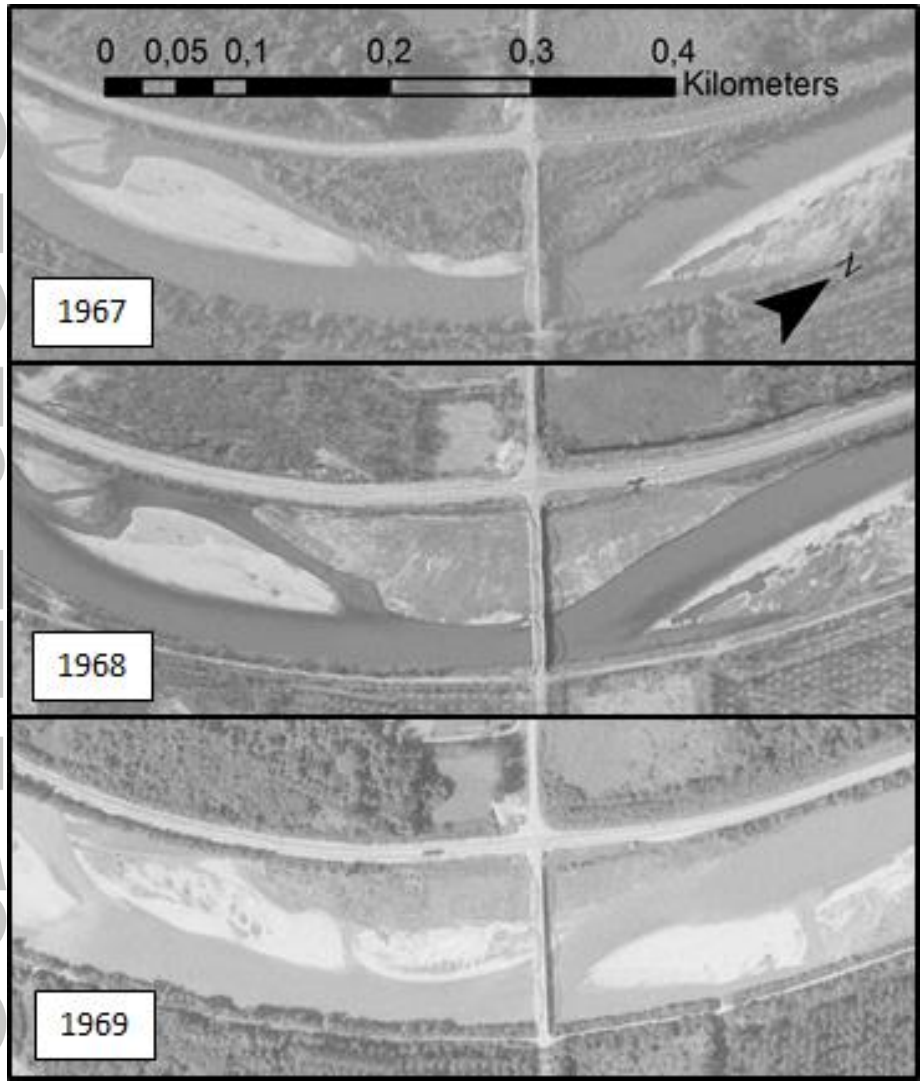

Figure 3: Three aerial images showing the same bar fully vegetated (1967), after vegetation and sediment removal (1968), and a year later showing rapid early vegetation recovery (1969) at pont de Gresy, Aiton (km 7 of the study reach, flow right to left). Note that the dark shade of the entire surface of the bar beneath the bridge in the 1968 image is a result of vegetation and bar surface excavation and, therefore, shows complete removal of the vegetation cover on the bar during 1968. (source images: Institut Géographique National)

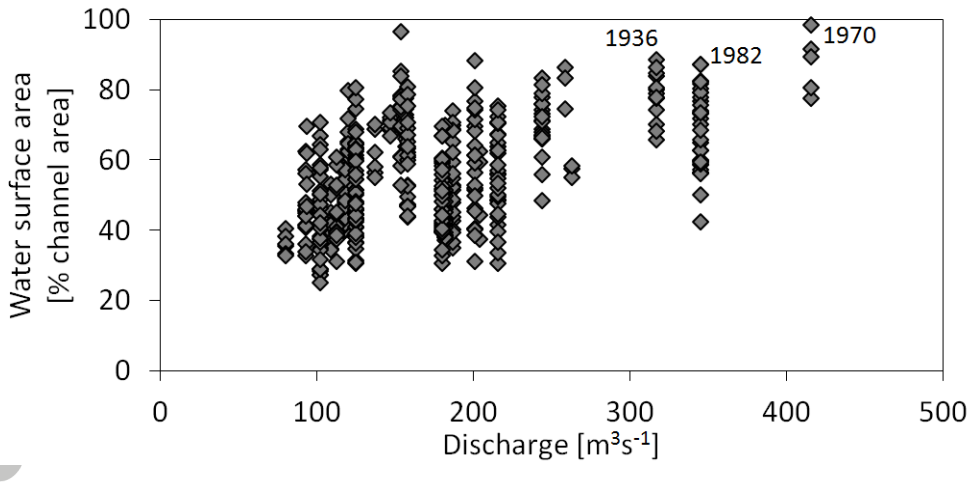

Figure 4: Percentage of the embanked channel area occupied by water within the 1 km sections of the study reach captured by the available aerial images, plotted in relation to the daily discharge monitored at Grenoble on the day of image capture. (Note that not all sets of images cover the entire set of 33 1km sections)

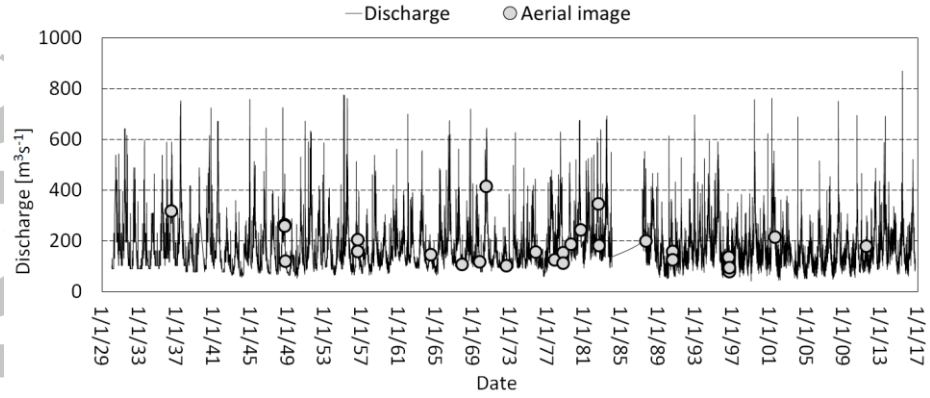

Figure 5: Daily mean discharge at Grenoble, locating the times when the analysed aerial images were captured (note that high discharges, particularly those above 600 $m^3 s^{-1}$, are over-estimated in the records before 1960).

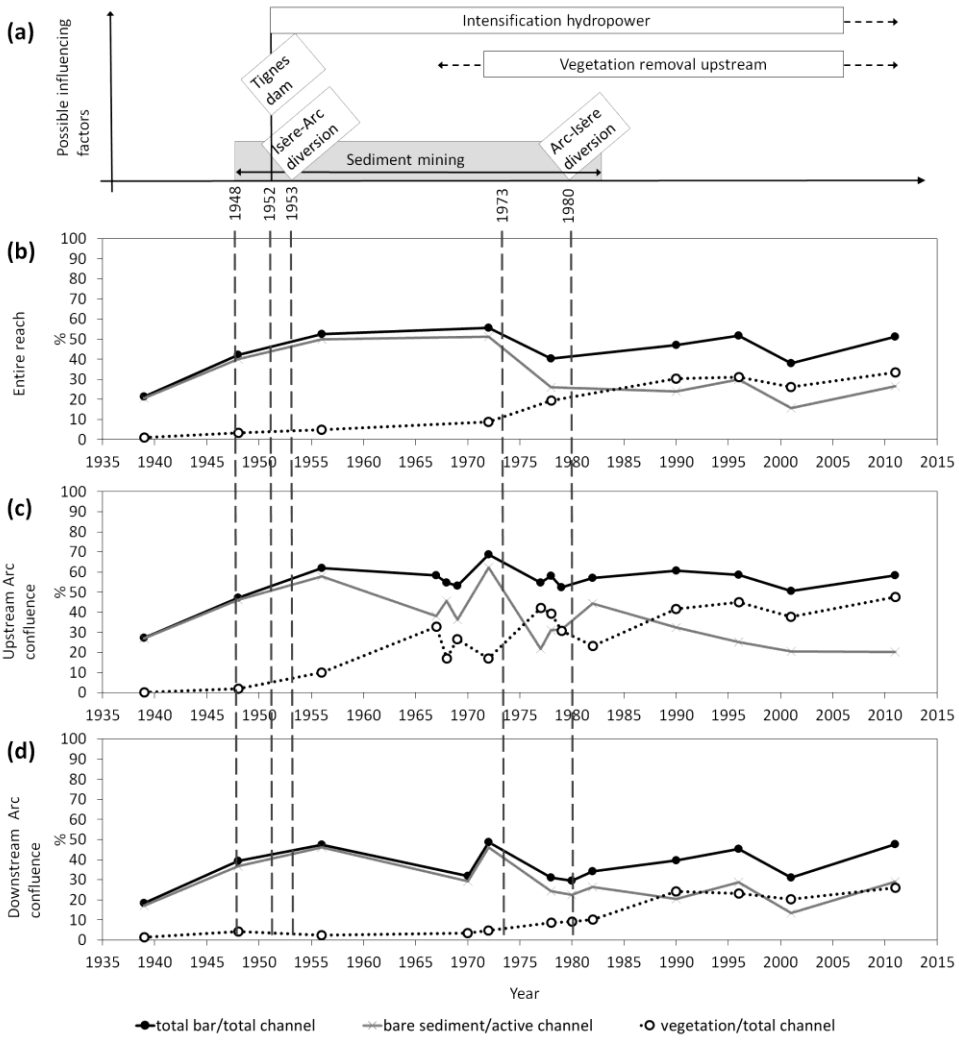

Figure 6: Percentage of embanked channel occupied by bars (exposed bare sediment and vegetated surfaces) and vegetated bars (vegetated surfaces only); and percentage of the active channel (water and exposed bare sediment) occupied by bars (exposed bare sediment) extracted from aerial images of different date covering (b) the entire 33 km study reach; (c) the study reach upstream of the River Arc confluence; and (d) the study reach downstream of the River Arc confluence. Data are presented for all image dates that provide complete or near-complete coverage of the relevant reach. The timing of implementation of the main human factors that may have influenced the biogeomorphic changes are indicated in (a), with the commencement of sediment mining, the activation of the Tignes hydropower dam, and the Isère-Arc and Arc-Isère diversions marked by vertical dashed lines.

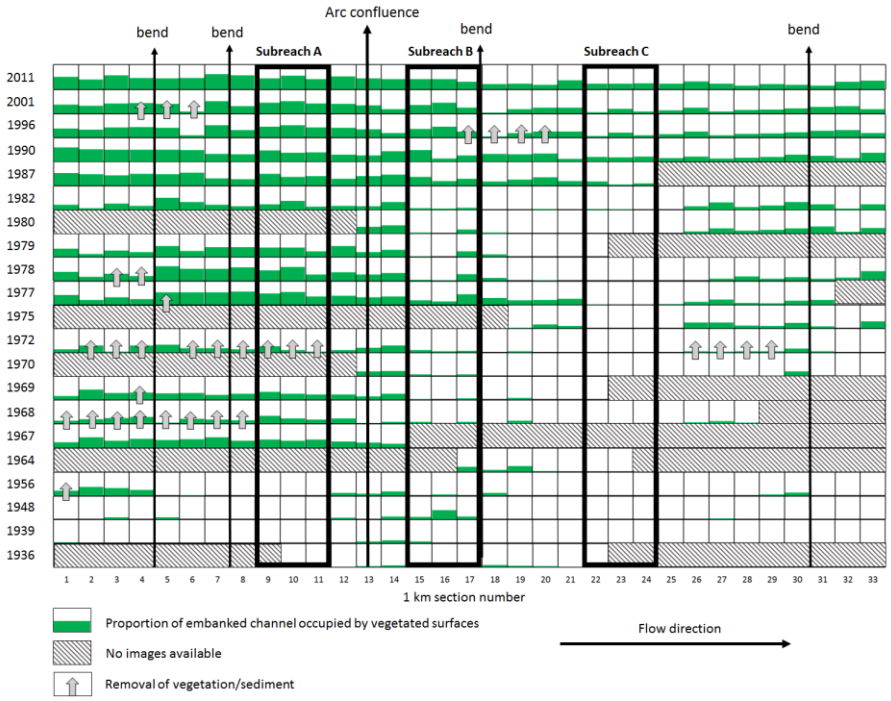

Figure 7: Proportion of the embanked channel area that is vegetated in each of the 1 km sections of the study reach extracted from aerial images of different date. The positions of three 3 km sections (subreaches A, B and C) are shown, where a detailed analysis of bar dimensions and migration was undertaken

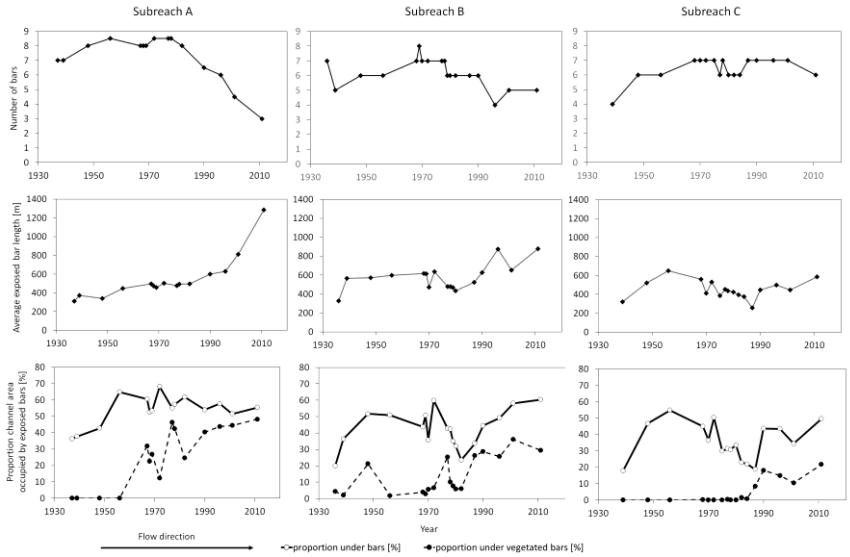

Figure 8: The number, length and area (total and vegetated) of bars within the embanked channel in subreaches A, B and C. Data are drawn from all images providing full coverage of each sub-reach.

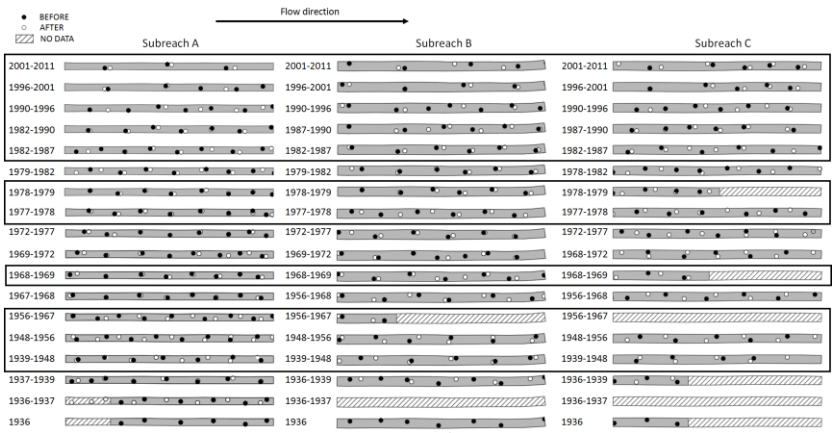

Figure 9: The changing position of exposed bar centroids between different start dates (black dots) and end dates (white filled dots). When both the start and end dates are identical for all three subreaches, the subreach maps are enclosed in a box.

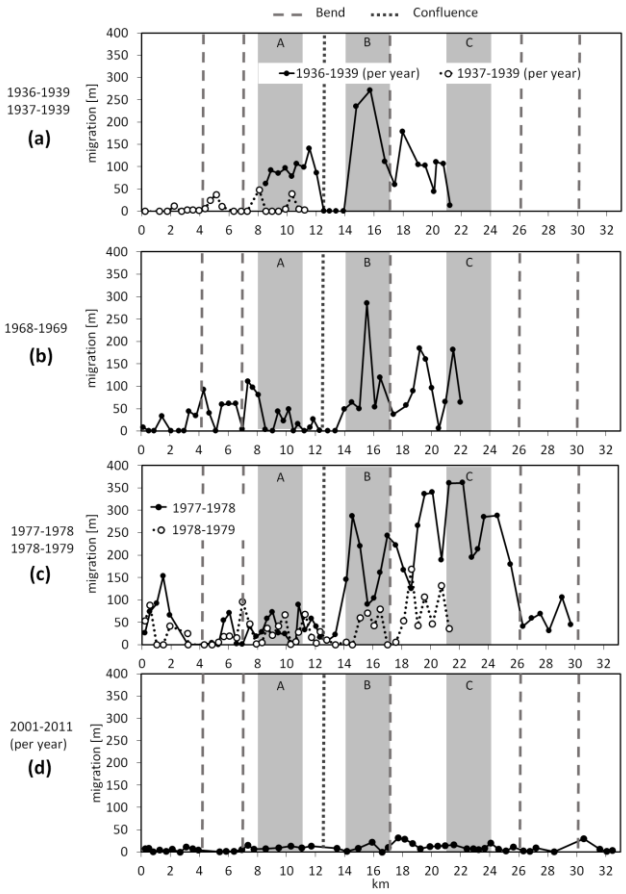

Figure 10: Annual (average for 1936-1939) downstream migration of exposed bar centroids at three different dates along the 33 km study reach from upstream (left) to downstream (right).

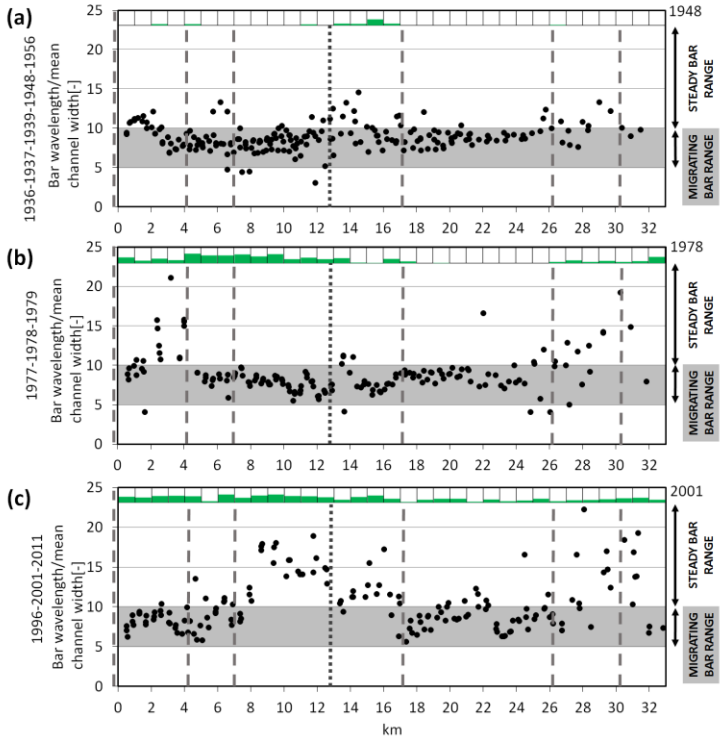

Figure 11: The ratio of bar wavelength to width along the 33km study reach extracted from images captured in (a) 1936, 1937, 1939, 1948 and 1956, (b) 1977, 1978, 1979 and (c) 1996, 2001, 2011. The vegetated proportion of the embanked channel in each 1 km subreach is indicated above each graph and the location of the Arc confluence and major bends in the channel are indicated, respectively, by a short-dashed and long-dashed vertical lines. The grey band on each graph represents the range of bar wavelength/width values expected from bar theory for migrating bars, whereas steady bars would be expected to plot well above the grey band.

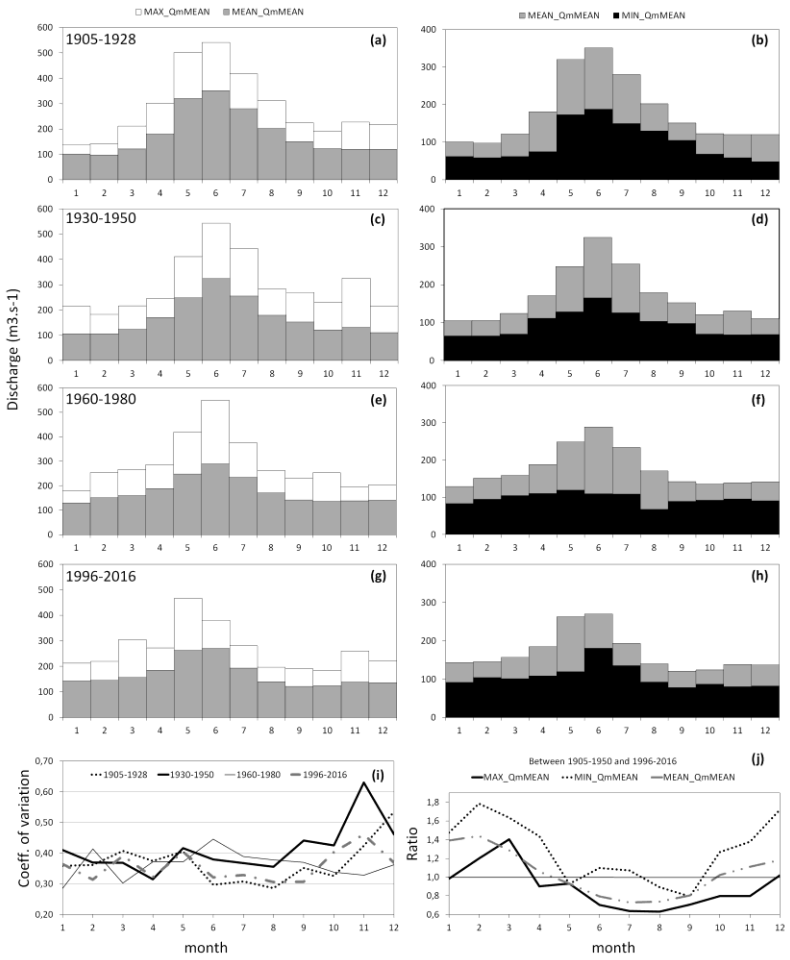

Figure 12: The upper four pairs of graphs (a,b; c,d; e,f; g,h) illustrate the average for each calendar month (MEAN_QmMEAN) of series of mean monthly discharges (QmMEAN – estimated from the daily flow record) observed within four different time periods (1905-1928 (24 years), 1930-1950 (21 years), 1960-1980 (21 years), 1996-2016 (21 years)) and plotted against the maximum average monthly flow (MAX_QmMEAN) in the graphs on the left and the minimum average monthly flow (MIN_QmMEAN) in the graphs on the right. Graph (i) illustrates the coefficient of variation of monthly flows within each month and four time periods and graph (j) illustrates the ratio of the MAX_QmMEAN, MIN_QmMEAN and MEAN_QmMEAN in 1905-1950 to that in 1996-2016.

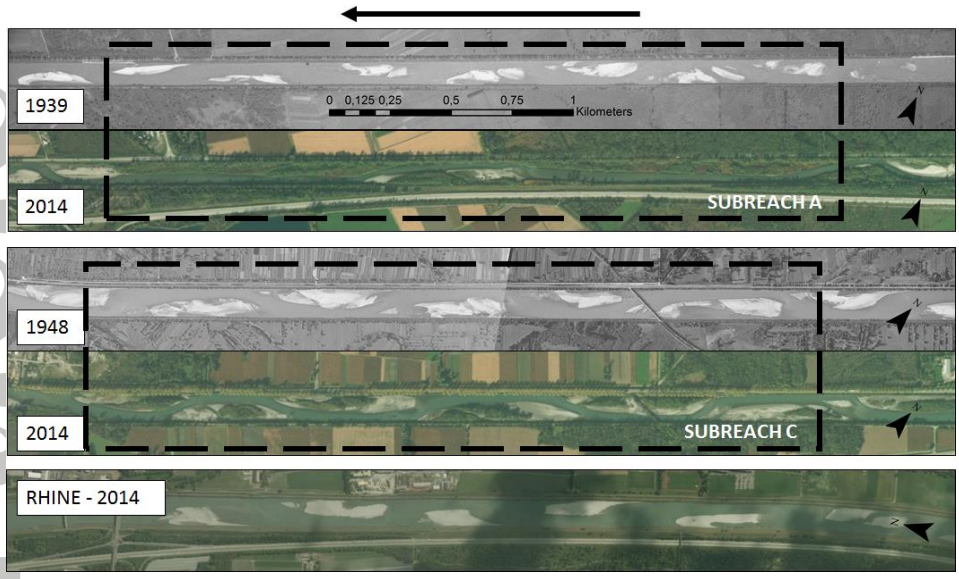

Figure 13: Images of subreach A in 1939 and 2014, subreach C in 1948 and 2014, and a similar length section of the embanked River Rhine in 2014 (source images 1939 and 1948: Institut Géographique National; source images 2014: Esri, DigitalGlobe, GeoEye, Earthstar Geographics, CNES/Airbus DS, USDA, USGS, AEX, Getmapping, Aerogrid, IGN, IGP, swisstopo, and the GIS User Community)

BIOMORPHODYNAMICS OF ALTERNATE BARS IN A CHANNELIZED, REGULATED RIVER: AN INTEGRATED HISTORICAL AND MODELLING ANALYSIS

Alyssa J. Serlet[1,2,*], Angela M. Gurnell[2], Guido Zolezzi[1], Geraldene Wharton[2], Philippe Belleudy[3], Camille Jourdain[3]

[1] Dept. of Civil Environmental and Mechanical Engineering, University of Trento, Trento, Italy

[2] School of Geography, Queen Mary University of London, London E1 4NS, United Kingdom

[3] Univ. Grenoble Alpes, CNRS, IRD, Grenoble INP, IGE, F-38000 Grenoble, France

* corresponding author

KEY FINDINGS

- Detailed historical and modelling analysis in a 33 km reach of Isère River over 80 years
- Trajectories of channel planform change in morphology and vegetation and linked to potential causes
- Shift from unvegetated migrating alternate bars to vegetated steady bars